

Petrology, geochemistry and tectono-magmatic affinity of gabbroic olistoliths from the ophiolite mélange in the NW Dinaric-Vardar ophiolite zone (Mts. Kalnik and Ivanščica, North Croatia)



†Boško Lugović¹, Damir Slovenec², Ralf Schuster³, Winfried H. Schwarz⁴ and Marija Horvat²

¹ University of Zagreb, Faculty of Mining, Geology and Petroleum Engineering, Department of Mineralogy, Petrology and Mineral Resources, Pierottijeva 6, 10000 Zagreb, Croatia

² Croatian Geological Survey, Sachsova 2, 10000 Zagreb, Croatia;
(corresponding author e-mail: damir.slovenec@hgi-cgs.hr)

³ Geological Survey of Austria, Neulinggasse 38, 1030 Vienna, Austria

⁴ Institute of Earth Sciences, Im Neuenheimer Feld 234-236, 69120 Heidelberg, Germany

doi: 10.4154/gc.2015.03

Geologia Croatica

ABSTRACT

Mafic intrusive rocks are subordinately represented fragments of the oceanic crust in the ophiolite mélange exposed at Mts. Kalnik and Ivanščica located in the NW Dinaric-Vardar ophiolite zone. This ophiolite mélange occurs in the northern area of the Kalnik Unit and represents the SW surface boundary of the Zagorje-Mid-Transdanubian Shear Zone. The mélange, except for mafic intrusive rocks, consists of a chaotic mixture of various extrusive rocks formed in different tectonic settings of the Repno Oceanic Domain (ROD). The ROD was the segment of Neo-Tethys that connects the Meliata-Maliak and Dinaric-Vardar oceanic systems. Previous study of mafic extrusive sequences suggested an 80 Ma period of tectono-magmatic evolution of the ROD from intra-continental rifting during the Anisian, to the formation of proto-arc crust during the Callovian-Oxfordian. The domain exposes ophiolitic rocks in four mélange areas. Isotropic gabbroic rocks that are abundant in two northern areas (Mts. Kalnik and Ivanščica), can be discriminated into three distinct geochemical groups: (A) N-MORB-type gabbro [(Th/Nb)_n = 0.99–1.10; (Nb/La)_n = 0.95–0.99], (B) IAT-type amphibole gabbro with clear supra-subduction characteristics [(Th/Nb)_n = 6.04–8.16; (Nb/La)_n = 0.32–0.42] and (C) BABB-type amphibole-bearing gabbro [(Th/Nb)_n = 2.88–4.02; (Nb/La)_n = 0.58–0.69]. Representative gabbro samples of each geochemical group were dated by the Ar-Ar and/or the K-Ar dating method. The Early Jurassic N-MORB-type gabbros (geochemical group A), ~185 Ma old, signifies a peculiar stage of Palaeo-Tethyan slab break-off. The Late Jurassic IAT-type gabbros (geochemical group B), ~147 Ma old, is the vestige of a nascent intra-oceanic arc, whilst the Early Cretaceous BABB-type gabbros (geochemical group C), ~100 Ma old, provides evidence of magmatism in the back-arc marginal basin. The analyzed gabbroic rocks enable refinement and completion of the geodynamic evolution of the ROD, from the opening of an ensialic back-arc basin during the Ladinian and a continuous spreading event until the Bajocian. Intra-oceanic convergence was initiated in the Bathonian, with the formation of a nascent island-arc during the Tithonian, leading to formation of a Cretaceous ensimatic back-arc marginal basin. There are many lines of evidence that correlate the geodynamic evolution of the ROD with the Albanide-Hellenide Neo-Tethyan oceanic segment.

Keywords: petrology and geochemistry, N-MORB, IAT, BABB, gabbro, ophiolite mélange, Dinaric-Vardar ophiolite zone, Mts. Kalnik and Ivanščica, Croatia

1. INTRODUCTION

The oceanic lithosphere may be preserved as large thrust sheets of a relatively undisturbed coherent lithostratigraphic pile (ophiolite complex) thrust onto a tectono-sedimentary unit which represents a chaotic mixture of various (in terms of age and lithology), ophiolitic rock fragments, embedded in a matrix during accretion, obduction and emplacement onto the continental margin (ophiolite *mélange*). Ophiolite *mélanges* are by consensus understood as chaotic tectono-sedimentary complexes initially deposited by tectonically induced sedimentary processes in the deep ocean trench (accretionary wedge) from a fore-arc region over the subducting plate in front of the leading edge of the overriding plate (FESTA et al., 2010). Consequently, the *mélange* mostly incorporates very heterogeneous magmatic material, derived from both interfaced oceanic sides of the accretionary wedge, representing remnants of different tectonostratigraphic units formed during the lengthy evolution of an oceanic system. Many *mélanges* are overlain by slices of coherent fragments of the genetically related oceanic lithosphere (ophiolites) which may include lithologies not found in the associated *mélange* and vice versa (eg. WAKABAYASHI & DILEK, 2003). Only the systematic petrological and geochemical analyses of ophiolite thrust sheets and magmatic rock fragments archived in the associated *mélanges* provide the opportunity to study the history of an oceanic system in order to understand the complete geodynamic evolution of an ancient oceanic domain; from intracontinental rifting, onset of oceanization and formation of oceanic lithosphere, through spreading and convergence until the closure and final ophiolite emplacement. Such systematic studies are particularly useful when regional field relationships fail in areas of poorly exposed ophiolitic rocks such as the Sava Zone or the Pannonian Basin.

In the SW segment of the Zagorje-Mid-Transdanubian shear Zone (ZMTDZ), i.e. in the northeasternmost border of the Sava-Vardar Zone (SVZ) a tectono-sedimentary ophiolite *mélange* is observed in the form of separate areas outcropping and forming the slopes of Mts. Kalnik, Ivanščica, Medvednica & Samoborska Gora (e.g. PAMIĆ & TOMLJENOVIC, 1998; with references; Fig. 1A). All these *mélange* areas are integrated as a single tectonostratigraphic unit named by HAAS et al. (2000) as the Kalnik Unit (Fig. 1B). On account of similar textural features, all the *mélange* areas of the Kalnik Unit provide strong evidence for a discrete Mesozoic oceanic domain called the Repno Oceanic Domain (ROD - sensu BABIĆ et al., 2002). The ROD was a part of the Neo-Tehtys Oceanic realm and links the Meliata-Maliak and Dinaric-Vardar oceanic domains (BABIĆ et al., 2002; Fig. 1C). This may be understood to represent the key oceanic domain connecting the Central Dinaridic ophiolites located to the SW, with Meliata-Maliak ophiolites to the NE and the Alpine ophiolites to the NW (SLOVENEK & LUGOVIĆ 2008, 2009; SLOVENEK et al., 2010, 2011). The ROD is documented mainly by isolated bodies of extrusive rocks, whereas coherent fragments of oceanic lithosphere (ophiolite complexes) are lacking. It contains four separate ophiolite *mélange* areas in two southern (Mts. Medvednica and Samoborska Gora), and two northern parts (Mts. Ivanščica and Kalnik) (Fig. 1A-

B). Extensive studies of extrusive rocks, particularly the pillow-basalts associated with radiolarian cherts from all four *mélange* areas (SLOVENEK & LUGOVIĆ, 2009, 2012; SLOVENEK et al., 2010, 2011; KISS et al., 2012), and intrusive gabbroic rocks from the Mt. Medvednica ophiolite *mélange* (SLOVENEK & LUGOVIĆ, 2008), provided a high-resolution view of the geodynamic evolution of the ROD that commenced with intra-continental rifting during Anisian time. This was followed by the formation of the proto-oceanic crust, followed by the onset of spreading and maximum widening of the oceanic domain in the Bajocian, until the formation of an infant proto-arc crust in the Callovian-Oxfordian.

In many *mélange* portions, extrusive rock sequences are generally the most abundant fragments. However, subordinate blocks of intrusive gabbroic rocks can also be an excellent magmatic indicator of a geotectonic setting. Although the hectometre-scale gabbroic blocks are relatively abundant in the Kalnik and Ivanščica Mts. *mélange* areas of the ROD (Fig. 2A-B), they have not been previously investigated in detail. The gabbroic rocks from the Kalnik and Ivanščica Mts. *mélange* are dated here by Ar-Ar and/or K-Ar dating methods and can be geochemically and petrologically categorized into three distinct groups. Therefore, they can represent different geotectonic formational settings that were not recognized in previous research.

The aim of this work is to provide an overall petrological and geochemical characterization of the Mt. Kalnik and Ivanščica gabbroic rocks to determine their petrogenesis and to propose a likely geotectonic setting for their formation, with the purpose of improving and completing our knowledge of the geodynamic evolution of the ROD as a discrete Mesozoic domain that was the corner-stone between the Meliata-Maliak and Dinaric-Vardar oceanic systems. The Kalnik and Ivanščica Mts. gabbroic rocks are correlated with equivalent rocks from the nearby Mt. Medvednica highlighting their potential geotectonic link. With reference to the chronology of particular tectonomagmatic episodes, the inferred geodynamic model for the ROD in many respects correlates with the model for the Albanide-Hellenide Neo-Tethyan ocean segment, as deduced from the study of ophiolites and ophiolite *mélanges* in the latter area (SACCANI et al., 2011).

2. REGIONAL GEOLOGICAL SETTING

Geographically the study area is located in the northernmost part of the Dinarides, located between the Adriatic Sea and the Southern Alps in the southwest and west and the Pannonian Basin with some inselbergs in the north and east (Fig. 1A-B). The Dinarides represent an Alpine fold-thrust belt, bordered to the southwest by the Adriatic (Apulian) microplate, the Southalpine and Austroalpine Unit to the north and by the Tisza Mega-Unit to the east (HAAS et al., 2000; Fig. 1B). They are subdivided into the External Dinarides, mainly consisting of Mesozoic carbonate platforms (VLAHOVIĆ et al., 2005), and the Internal Dinarides which comprise several zones: The Bosnian flysch zone is overlain by a zone composed of Upper Jurassic to Cretaceous mixed carbonate and siliciclastic sedimentary units, derived from a distal

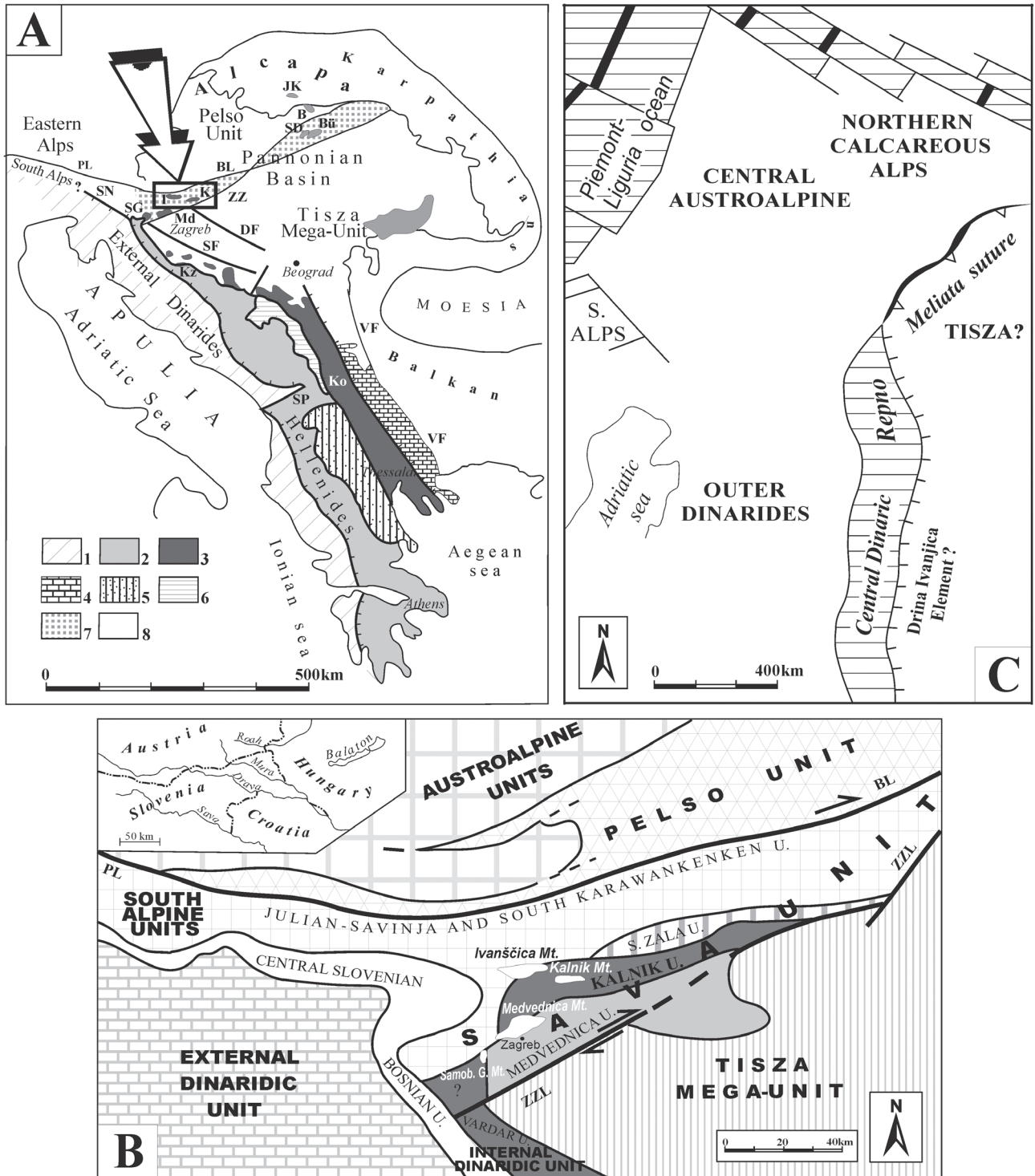


Figure 1: (A) Geotectonic sketch map of the Alps, Dinarides and Hellenides showing the position of the Periadriatic-Sava-Vardar suture zone (after PAMIĆ, 2000). Legend: 1 – External units (External Dinarides and Alps); 2 – Internal units [Passive continental margin, Central Dinaride Ophiolite Belt (CDOB), Miirdita Zone]; 3 – Periadriatic-Sava-Vardar Zone; 4 – Serbo-Macedonian Massif; 5 – Pelagonides; 6 – Golija Zone; 7 – Zagorje-Mid-Transdanubian Zone; 8 – Pannonian Basin. Faults: BL – Balaton; DF – Drava; PL – Periadriatic Lineament; SF – Sava Fault; SP – Scutari-Peć; SN – Sava Nape; VF – Vardar; ZZ – Zagreb-Zemplin. Mountains: I – Ivanščica; K – Kalnik; Ko – Kopaonik; Kz – Kozara; Md – Medvednica; SG – Samoborska Gora; SD – Szarvaskő-Darnó; Bü – Bükk. B – Bódva valley; JK – Jaklovce. (B) Sketch map of the structural units and major lineaments (modified after HAAS et al., 2000). Insert map: geographic setting of the area presented in the sketch map. Legend: BL – Balaton Lineament; ZZL – Zagreb-Zemplin Lineament; PL – Periadriatic Lineament. (C) Sketch map of hypothetical reconstruction of the oceanic belt consisting of Meliata, Repno and Central Dinaric Ophiolite Zone segments (after BABIĆ et al., 2002).

Adriatic plate margin, which was involved in the Late Jurassic ophiolite obduction. Most internal units comprise the Central Dinaridic Ophiolite Zone (CDOZ) and finally the Sava-Vardar Suture Zone (SVSZ) sensu PAMIĆ (2002). The

Dinarides characteristically stretch northwest-southeast and were traditionally understood to be bracketed between the Zagreb-Zemplin Lineament and the Skutari-Peć transform fault (eg. PAMIĆ, 2002; Fig. 1A).

The study area comprises the southwestern part of a larger zone, about 100 km wide and 400 km long, sheared between two regional fault systems, the Zagreb-Zemplin Lineament to the south and the Periadriatic-Balaton Lineament to the north, which was (after PAMIĆ & TOMLJENOVIC, 1998), recognized as the ZMTDZ (Fig. 1A-B). This area forms a junction between the Southalpine and Austroalpine Unit, the Tisza Mega-Unit and the Internal Dinarides. It is also known as the Sava Unit (HAAS et al., 2000; Fig. 1B). The ZMTDZ includes triangular shaped intra-Pannonian inselbergs: Mts. Kalnik, Ivanščica, Medvednica and Samoborska Gora. The inselbergs are composed of pre-Neogene heterogeneous and superimposed Dinaric and Alpine tectonostratigraphic and tectonometamorphic units, (see for example: PAMIĆ & TOMLJENOVIC, 1998; TARI & PAMIĆ, 1998; HAAS et al., 2000; HAAS & KOVÁCS, 2001; PAMIĆ, 2002). However, the origin of these units is still debated. Structural and palaeomagnetic data indicate that the pre-Neogene basement of Mts. Ivanščica, Kalnik and Medvednica experienced large, regional-scale tectonic transport from the northwest, and an approximately 130° clockwise rotation during the Oligocene to the earliest Miocene (TOMLJENOVIC et al., 2008), that aligned them almost perpendicular to the overall northwest – southeast Dinaric structural trend. When reconstructed for this clock-wise rotation, these three mountains continue the main Dinaric trend to the northwest. On the basis of their similar tectonostratigraphic evolution, SCHMID et al. (2008) considered the ZMTDZ to be part of the Western Vardar Ophiolite Unit.

The Kalnik and Ivanščica Mts. ophiolite mélange (Figs. 2A and B) form the two separate northern mélange areas of the Kalnik Unit (Fig. 1B). The Kalnik Unit consists of the lithological remnants of a discrete oceanic domain that connects the Dinaric-Vardar ophiolites, located to the southwest, with the Meliata-Maliak ophiolites exposed to the northeast. Based on matrix palynomorph assemblages, the accretionary age of the Kalnik Unit, i.e. ophiolite mélange is inferred to be Middle Jurassic to Hauterivian (BABIĆ et al., 2002). This time interval represents a period of accumulation of lithostratigraphically diverse material in the intra-oceanic trench (SLOVENEK et al., 2011).

The Kalnik Unit was involved in Aptian to post-Palaeocene emplacement onto the eastern continental margin of the Adria plate (PAMIĆ & TOMLJENOVIC, 1998; PAMIĆ, 2002). However, the basement rocks of the Kalnik Unit in the Ivanščica and Kalnik Mts. are not known. In Mt. Medvednica, the Kalnik Unit is thrust onto Aptian low-grade metamorphic complexes (Medvednica Unit, HAAS et al., 2000; Fig. 1B), generated during the emplacement of the Late Jurassic island-arc onto the Adria continental margin (LUGOVIĆ et al., 2006). However, the pelitic to silty matrix of the Kalnik Unit does not show a metamorphic overprint from burial diagenesis (JUDIK et al., 2008).

3. LOCAL GEOLOGY AND DESCRIPTION OF THE STUDY AREA

A simplified geological map of the Kalnik and Ivanščica Mts. is shown in Figures 2A and 2B, respectively. The old-

est rocks in the area are Middle-Upper Triassic limestones and dolomites derived from the Adriatic passive continental margin (ŠIMUNIĆ et al., 1982; HALAMIĆ, 1998). At Mt. Ivanščica, this carbonate succession is intersected by calc-alkaline extrusives and interlayered with distal pyroclastics, interpreted as remnants of a late Anisian-Ladinian Andean-type volcanic arc, located at the European continental margin (GORIČAN et al., 2005). Late Jurassic to Early Cretaceous limestones unconformably overlie this Middle Triassic volcano-sedimentary formation. Both units are in turn overthrust onto an ophiolite mélange.

These Mesozoic rock successions have not been encountered at Mt. Kalnik. The central ridge of Mt. Kalnik consists of Palaeocene carbonate breccias thrust over Neogene sedimentary rocks (ŠIMUNIĆ et al., 1981). The common constituents of these breccias are fragments of Triassic algal and stromatolitic limestones and dolomites, as well as Jurassic and Upper Cretaceous limestones. Similar breccias are also found in nearby Mt. Medvednica (ŠIMUNIĆ et al., 1993), and were encountered during drilling in the Drava Depression (ŠIMUNIĆ & PAMIĆ, 1989) suggesting a wide areal extent.

Several individual fragments of highly serpentinized mantle peridotites (lherzolites) were exhumed at the mountain ridge tectonic zone (POLJAK, 1942), together with a composite block of serpentinized lherzolite underlain by metamorphic sole amphibolites (LUGOVIĆ et al., 2007). The amphibolites were dated by K-Ar on amphibole separates which yielded an age of 118 ± 8 Ma (IGNJATIĆ, 2007). The northern part of the Mt. Kalnik ophiolite mélange is thrust onto the Neogene-Pleistocene sedimentary succession (ŠIMUNIĆ et al., 1982). All other contacts of the ophiolite mélange areas of Mts. Kalnik and Ivanščica exhibit a tectonic-erosional unconformity against the youngest Neogene and Pleistocene sedimentary rocks (Fig. 2A-B).

The ophiolite mélange areas of Mts. Kalnik and Ivanščica show similar structural features characterized by a “block-in-matrix” fabric, typical of chaotic complexes from subduction-related tectonic mélanges (FESTA et al., 2010). They are dominated by magmatic rocks and contain lithostratigraphically heterogeneous fragments of sedimentary rocks including greywacke, minor shale, red and grey cherts, and scarce limestones (ŠIMUNIĆ et al., 1982). The fragments range in size from pebbles to hectometre-kilometre sized blocks embedded in a predominantly sheared continent-derived pelitic to silty matrix (Figs. 2A-B). Fragments of mafic extrusive rocks are the prevailing magmatic lithologies in both ophiolite mélange areas. They show various geochemical signatures consistent with their different geotectonic formational settings during an age span from the Illyrian to the late Oxfordian (SLOVENEK et al., 2011). Gabbroic rocks are relatively abundant in the mélange areas of Mts. Kalnik and Ivanščica and occur as hectometre-sized homogeneous blocks (CRNKOVIĆ et al., 1974; VRKLJAN, 1989; PAMIĆ, 1997; VRKLJAN & GARAŠIĆ, 2004; Fig. 2A-B). However, an exceptional composite gabbro block, intersected by a metre-wide dacitic dyke was observed in Gotalovec quarry at Mt. Ivanščica. In the field, part of these Cretaceous blocks

(Fig. 2A, location 3 and Fig. 2B, location 3) appear as fault-bounded tectonic inclusions subsequently embedded in the mélangé during the ophiolite emplacement. The locations of the all analysed blocks are indicated in Figure 2A for Mt. Kalnik and Figure 2B for Mt. Ivanščica.

4. ANALYTICAL TECHNIQUES

The mineral compositions of ten samples were analysed at the Mineralogisches Institut der Universität Heidelberg, Germany, using a CAMECA SX51 electron microprobe equipped with five wavelength-dispersive spectrometers. Measurements were performed using an accelerating volt-

age of 15 kV, a beam current of 20 nA, beam size of $\sim 1 \mu\text{m}$ (for feldspars $10 \mu\text{m}$) and 10s counting time for all elements. Natural oxides and silicates were used as standards and for calibration. Raw data were corrected for matrix effects with the PAP algorithm (POUCHOU & PICHOR, 1984, 1985) implemented by CAMECA. Calculations of the structural chemical formulae were undertaken using a software package written by Hans-Peter Meyer (Mineralogisches Institut, Heidelberg).

Bulk-rock powders for chemical analyses of 21 samples were obtained from vein-free rock chips. The samples were analysed by ICP-OES for major elements and ICP-MS for

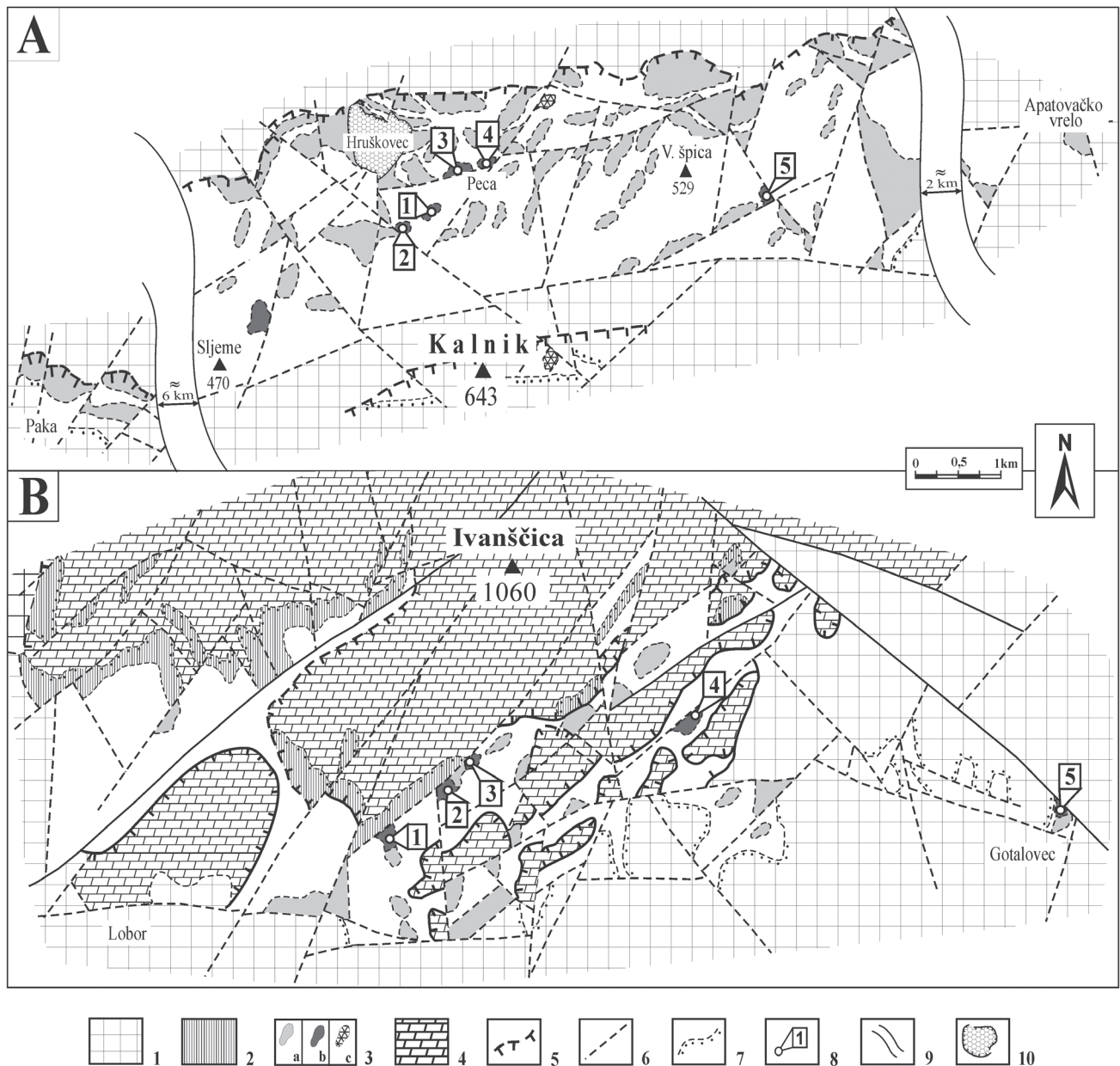


Figure 2: (A) Simplified geological map of Mt. Kalnik and (B) of Mt. Ivanščica (modified after ŠIMUNIĆ et al., 1982 and HALAMIĆ, 1998). Legend: 1 – Neogene and Pleistocene sedimentary rocks; 2 – Jurassic-Cretaceous limestones; 3 – ophiolite mélangé with blocks of: 3a – basalt, 3b – gabbro, 3c – tectonite peridotite and Triassic-Jurassic radiolarites, sandstones and shales (not separated on the maps); 4 – Triassic limestones and dolomites; 5 – reverse or thrust faults; 6 – normal faults; 7 – discordance line, tectonic-erosion discordance; 8 – sample location (Mt. Kalnik: 1 = vsk-242/2, vsk-242/4, vsk-242/6; 2 = vsk-204; 3 = vsk-229/1, vsk-229/7, vsk-229/12; 4 = vsk-228, vsk-228/2, vsk-228/5; 5 = vsk-217/1; Mt. Ivanščica: 1 = be-3; 2 = vsi-5; 3 = vsi-8/1, vsi-8/2; 4 = vsi-7/1; 5 = gi-2, gi-5, gtc-3, gtc-4, gtc-6); 9 – picture break; 10 – quarry.

all trace elements, utilizing the 4Lithoresearch analytical protocol at Activation Laboratories in Ancaster, Canada. Major element and trace element concentrations were measured with accuracy better than 1% and 5%, respectively.

Isotopic compositions of six bulk rock samples were measured in the Centre de Recherches Pétrographiques et Géochimiques in Vandoeuvre, France on a Triton Plus mass spectrometer. Normalizing ratios of $^{86}\text{Sr}/^{88}\text{Sr} = 0.1194$ and $^{146}\text{Nd}/^{144}\text{Nd} = 0.7219$ were used. The $^{87}\text{Sr}/^{86}\text{Sr}$ ratio for the NBS 987 Sr standard based on $n = 92$ for the period of measurement was 0.710242 ± 0.000030 (2σ). The $^{143}\text{Nd}/^{144}\text{Nd}$ ratio for the La Jolla standard was 0.511845 ± 0.000010 (2σ) ($n = 22$). Total procedural blanks were ~ 500 pg and ~ 150 pg for Sr and Nd, respectively.

$^{40}\text{Ar}/^{39}\text{Ar}$ analysis was performed at the Institut für Geowissenschaften der Universität Heidelberg, Germany. The amphibole separate from the gabbro sample vsk-228 was prepared by crushing and sieving the 200–400 μm fraction followed by magnetic separation and finally by handpicking under a stereomicroscope. For irradiation, the samples were wrapped in Al-foil and packed into an evacuated and Cd-shielded quartz tube. They were irradiated for 15 days with $2 \cdot 10^{18}$ fast neutrons/ cm^2 . The irradiation was performed in the FRG-1 reactor of the Kernforschungszentrum Geesthacht, Germany. An apparent age and the flux gradients of the reactor were determined by an in-house muscovite standard; muscovite BMus/2, 328.5 ± 1.1 Ma, 1σ (SCHWARZ & TRIELOFF, 2007). Ar was extracted in a resistance-heated Ta furnace in a double-vacuum system up to 1400°C . The gas was cleaned using Zr-Al getters and a cooling trap. Ar isotope compositions were measured in a MAT GD-150 gas mass spectrometer with no detectable argon background. Constants used for age calculations are those recommended by STEIGER & JÄGER (1977) - note that suggestions for a revised decay constant for Ar-Ar dating (RENNE et al., 2010, 2011; SCHWARZ et al., 2011) would increase the apparent age by 1% in this age range. The argon amounts were corrected for blanks, decay and irradiation interference reactions. $^{40}\text{Ar}/^{39}\text{Ar}$ age uncertainties comprise the errors of the $^{40}\text{Ar}/^{39}\text{Ar}$ ratios of the irradiation monitors and age errors of the monitor. When two age uncertainties are given, the first error is without, while the error in parentheses is with monitor errors. All error assignments of argon isotopic ratios and ages given within this paper are within $\pm 1\sigma$, unless otherwise stated.

The K-Ar age data are measured on plagioclase separated from three gabbros (sample vsk-228/5, vsk-229/7 and vsi-8/1). Plagioclase was separated by an electromagnetic separator and standard heavy liquid techniques and finally was purified by hand picking under a stereomicroscope. The K concentration and Ar analysis were determined by ICP-OES and an isotope dilution procedure on noble gas mass spectrometry, respectively. The analyses were performed at the Activation Laboratories in Ancaster (Canada). The Ar analysis: Aliquot of the sample is weighted into an Al container, loaded into the sample system of the extraction unit, degassed at $\sim 100^\circ\text{C}$ over 2 days to remove the surface gases. Argon is extracted from the sample in a double vacuum fur-

nace at 1700°C . The Argon concentration is determined using isotope dilution with ^{38}Ar spike, which is introduced to the sample system prior to each extraction. The extracted gases are cleaned up in a two-step purification system. Then pure Ar is introduced into the custom built magnetic sector mass spectrometer (Reinolds type) with Varian CH5 magnet. The ion source has an axial design (Baur-Signer source), which provides more than 90% transmission and extremely small isotopic mass-discrimination. Measurement of Ar isotope ratios is corrected for mass-discrimination and then atmospheric argon is removed, assuming that ^{36}Ar is only from the air. The concentration of ^{40}Ar radiogenic is calculated using the ^{38}Ar spike concentration. After each analysis the extraction temperature is elevated to 1800°C for few minutes and the furnace is prepared for the next analysis. K-analysis: Aliquot of the sample is weighted into a graphite crucible with lithium metaborate/tetraborate flux and fused using a LECO induction furnace. The fusion bead is dissolved with acid. Standards, blanks and sample are analysed by an ICP Spectrometer.

5. PETROGRAPHY AND MINERAL CHEMISTRY

The studied gabbroic rocks are isotropic with preserved igneous fabric and show a non-cumulus anhedral granular texture with grain sizes of 1–3 mm and homogeneous structure. They were subdivided on the basis of their petrographic characteristics into three groups. The gabbros of group A are composed of plagioclase and augite, the gabbros of group B additionally contain variable edenitic amphibole, whilst edenite represents a minor phase in group C samples (Figs. 3A, B, C). Ilmenite and apatite occur as accessory minerals in all groups. Due to the textural relationships of edenite and its high content of TiO_2 , Al_2O_3 and Na_2O (up to 2.5, 8.3 and 2.7 wt%, respectively; Table 1) it is interpreted as an igneous mineral (compare with COOGAN, 2003), cotectic with augite (Table 2). These amphiboles have slightly different compositions compared to their Mt. Medvednica analogues which are classified as magnesiohornblende (Fig. 4). Some of the primary amphibole grains are partly altered to actinolite, ferroactinolite or ferro-anthophyllite (Table 1; Fig. 4). However, magnesiohornblende in the analysed gabbroic rocks may have formed during late crystallization of an evolved hydrous magma and may reflect the influence of a deep oceanic crustal hydrothermal system. The Gotalovec quarry gabbroic rocks (Fig. 2B, location 5; which are included in group C based on their geochemical similarities) are characterised by coarse grained intergranular textures and form a texturally unique group. They contain discrete domains of parallel oriented ilmenite plates (up to 35 μm wide) exsolved from completely decomposed mineral. A significant chemical difference with respect to the Mn-content of ilmenite was measured between rocks of groups B and C, (7.82–7.96 wt% vs. 3.28–4.67 wt% MnO), respectively. The representative gabbro (sample vsk-242/2) from group A contains low-Mn ilmenite (< 1.5 wt% MnO) typical of ocean ridge gabbros (HÉBERT et al., 1991). Plagioclase in gabbro samples of group A shows a nearly homogenous composition ($\text{An}_{\sim 50-45}$). However, magmatic plagioclase preserved

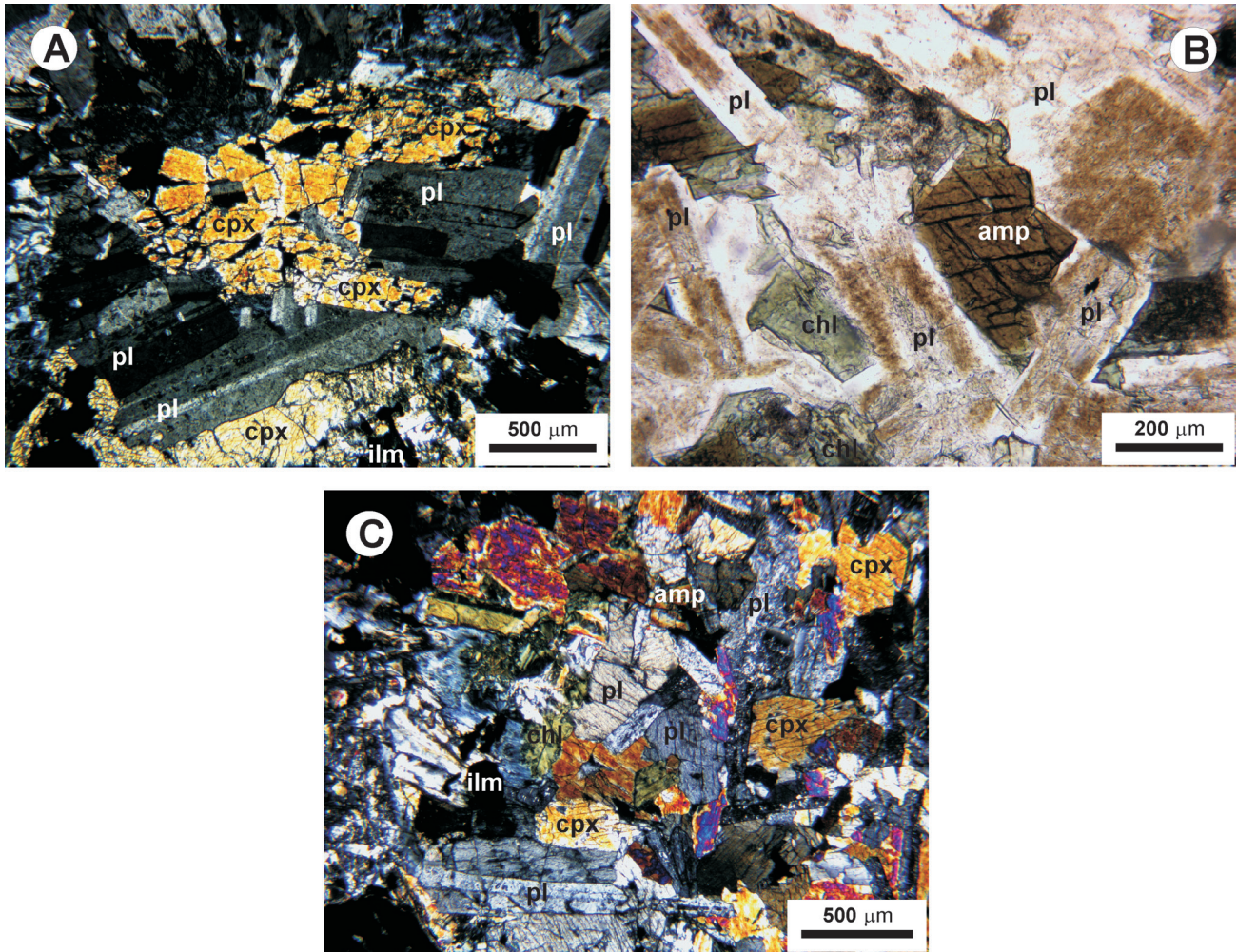


Figure 3: Microphotography of the Kalnik and Ivanščica Mts. non-cumulus gabbroic rocks subdivided on the basis of petrographic characteristics into three groups: (A) group A – composed of plagioclase and augite (sample vsk-242/2). N+, (B) group B – composed of plagioclase, augite and variable edenitic amphibole (sample vsk-228). N– and (C) group C – composed of plagioclase and augite while edenite represents a minor phase (sample vsk-229/12). N+. Legend: pl = plagioclase, cpx = clinopyroxene, amp = amphibole, ilm = ilmenite.

in rocks of groups B and C shows continuous normal zoning patterns with the widest core to rim compositional range of $An_{64.3}$ to $An_{33.7}$ measured in samples vsk-228 and vsk-228/5 and $An_{56.2}$ to $An_{36.8}$ measured in samples vsk-229/7 and vsi-8/2. A smaller portion of the measured feldspar shows an albite ($An_{0.3-2.9}$) to peristerite (An_{-6}) composition.

The dacite dyke intersecting gabbroic rocks in the Gotalovec quarry (Fig. 2B, location 5) shows a dense aphyric fine-grained pilotaxitic to intergranular texture. Close to the contact with the gabbro it may contain scarce clinopyroxene and albite phenocrysts. Clinopyroxene microphenocrysts are only partly replaced or pseudomorphed by ferroedenite/ferrohornblende corresponding to high temperature deuteric alteration, whereas chlorite, pumpellyite and titanite probably reflect hydrothermal alteration. The groundmass consists of albite laths, acicular clinopyroxene, interstitial quartz, ilmenite, chlorite and accessory pumpellyite, zircon, apatite and tourmaline.

Clinopyroxene composition is repeatedly used as an indicator of petrogenesis and geotectonic setting, particularly in ophiolites and other ocean-related rocks (BECCALUVA

et al., 1989). Selected clinopyroxene compositions from the analysed rocks are shown in Table 2, plotted in the classification diagram in Figure 5, and displayed in geochemical geotectonic discrimination diagrams in Figure 6.

The clinopyroxene from the gabbroic rocks of all groups is augite ($Wo_{36.5-44.7}En_{29.8-47.7}Fs_{11.0-29.7}$). In some samples augite is partly altered to trioctahedral (Type “I” of ZANE & WEISS, 1998) chlorite and belongs to the clinochlore-chamosite series. In all analysed samples clinopyroxenes show normal zoning patterns with continuously decreasing Mg# towards the rim of the crystal, the widest range of 85.4 to 65.7 was measured in the Gotalovec quarry sample gtc-4. This type and intensity of zoning is typical for slow cooling in a closed magmatic system (STERN, 1979). Dacite clinopyroxene has a low-Al ferroaugite composition ($Wo_{39.7-42.9}En_{16.8-26.9}Fs_{31.4-41.9}$). Both populations show a significant Fe-enrichment trend (Fig. 5; Table 2). The dacite clinopyroxene composition is typical for a highly evolved acidic magma as seen in Figure 6 where it occupies a position with the lowest Ti and highest Na-abundance.

Table 1: Selected microprobe analyses and formulae of amphibole from the gabbroic rocks and dacite in the Kaimik (KA) and Ivansčica (IV) Mts. ophiolite mélange.

Sample	Group B						Group C							
	vsk-228	vsk-228	vsk-228	vsk-228	vsk-229/1	vsk-229/7	be-3	vsi-5	+gtc-3	+gtc-3	+gtc-3	+gtc-3	+gtc-3	*gtc-6
Anal. nr.	1	2	26	27	1	12	13	3	3	17	34	40	57	19
Site	c	r	c	r	c	r	c	c	r	c	c	c	c	c
Mineral	Ed	Ed	Ed	Ed	Ed	Mhbl	Fath	Mhbl	Fed	Fact	Ed	Fhbl	Fath	Fed
Locality / Sample loc.	KA/4	KA/4	KA/4	KA/4	KA/3	KA/3	IV/1	IV/2	IV/5	IV/5	IV/5	IV/5	IV/5	IV/5
SiO ₂	43.80	46.30	44.99	47.47	45.68	49.52	49.2	48.91	48.11	47.81	47.18	47.58	49.97	47.70
TiO ₂	3.01	2.15	2.44	1.73	2.25	1.07	0.62	0.70	0.97	1.09	1.28	0.98	0.72	0.17
Al ₂ O ₃	9.54	7.42	8.28	5.50	7.29	3.26	1.63	5.24	3.20	2.98	5.33	3.32	1.07	2.92
Cr ₂ O ₃	0.02	0.06	0.04	0.05	0.01	0.10	0.03	0.00	0.00	0.00	0.00	0.03	0.02	0.00
FeO	16.12	16.81	17.48	19.47	18.92	20.90	33.19	14.14	26.37	28.65	18.87	28.94	33.68	29.94
MnO	0.34	0.27	0.29	0.05	0.33	0.28	0.37	0.34	0.44	0.46	0.43	0.38	0.56	1.03
MgO	11.56	12.35	11.46	11.10	10.73	10.26	17.29	14.42	8.23	6.97	11.95	6.70	8.52	5.08
CaO	10.24	10.31	10.07	9.98	9.81	9.80	4.17	11.55	8.54	8.15	9.60	8.00	2.65	7.78
Na ₂ O	2.90	2.24	2.66	2.08	2.53	1.45	0.59	0.89	1.53	1.26	2.04	1.14	0.47	1.87
K ₂ O	0.16	0.21	0.19	0.15	0.16	0.30	0.05	0.03	0.35	0.24	0.15	0.25	0.02	0.25
H ₂ O	2.01	2.02	2.01	2.00	1.99	1.98	1.91	2.02	1.94	1.92	1.98	1.91	1.92	1.89
Total	99.70	100.14	99.91	99.77	99.70	99.98	99.02	98.24	99.68	99.53	98.81	99.20	99.58	98.63
Si	6.617	6.914	6.793	7.188	6.951	7.599	7.767	7.221	7.482	7.501	7.173	7.486	7.810	7.686
Ti	0.342	0.242	0.277	0.197	0.258	0.124	0.074	0.078	0.113	0.129	0.146	0.116	0.085	0.021
Al	1.697	1.305	1.472	0.981	1.306	0.589	0.303	0.912	0.586	0.550	0.954	0.615	0.197	0.555
Cr	0.002	0.007	0.005	0.006	0.001	0.012	0.004	0.000	0.000	0.000	0.004	0.004	0.002	0.000
Fe ³⁺	0.000	0.000	0.000	0.000	0.000	0.000	0.000	0.230	0.000	0.000	0.000	0.000	0.000	0.000
Fe ²⁺	2.037	2.099	2.207	0.466	2.408	2.682	4.382	1.516	3.430	3.759	2.399	3.808	4.402	4.035
Mn	0.044	0.034	0.037	0.037	0.043	0.036	0.049	0.043	0.058	0.061	0.055	0.051	0.074	0.141
Mg	2.604	2.749	2.580	2.506	2.434	2.347	1.716	3.174	1.908	1.630	2.708	1.572	1.985	1.220
Ca	1.657	1.650	1.629	1.619	1.599	1.611	0.705	1.872	1.423	1.370	1.564	1.349	0.444	1.343
Na	0.850	0.649	0.779	0.611	0.746	0.431	0.181	0.255	0.461	0.383	0.601	0.348	0.142	0.584
K	0.031	0.040	0.037	0.029	0.031	0.065	0.010	0.006	0.069	0.048	0.029	0.050	0.004	0.051
Total	15.881	15.689	15.815	15.640	15.778	15.496	15.191	15.260	15.531	15.431	15.630	15.398	15.146	15.636
Mg#	56.1	56.7	53.9	50.4	50.3	46.7	28.1	64.5	35.7	30.3	53.0	29.2	31.1	23.2

Formulae calculated on the basis of 23 oxygens and fixed number of 15 cations excluding Na and K. Estimated H₂O corresponds 2 (OH) per formula unit. c = core, r = rim. Ed = edenite, Fed = ferro-edenite, Fhbl = ferro-hornblende, Mhbl = magnesio-hornblende, Fact = ferro-actinolite, Fath = ferro-anthophyllite. Mg# = 100*(Mg/(Mg + Fe²⁺)). + = diorite, * = dacite. Sample location number corresponds to the locations in Figure 2A-B.

Table 2: Selected microprobe analyses and formulae of clinopyroxene from the gabbroic rocks and dacite in the Kalinik (KA) and Ivanščica (IV) Mts. ophiolite mélange.

Sample	Group A			Group B			Group C														
	vsk-242/2	vsk-242/2	vsk-228	vsk-228	vsk-228	vsk-228	vsk-217/1	vsk-217/1	vsk-229/1	vsk-229/1	vsk-229/1	vsk-229/7	vsk-229/7	be-3	vsi-5	vsi-8/1	gtc-4	gtc-4	gtc-4	gtc-5	*gtc-6
Anal. nr.	2	5	13	14	17	17	19	20	37	38	14	15	3	3	19	4	3	4	4	9	9
Site	c	c	r	c	c	c	c	r	c	r	c	r	r	r	c	c	r	c	c	c	c
Locality / Sample loc.	KA/1	KA/1	KA/4	KA/4	KA/4	KA/4	KA/5	KA/5	KA/3	KA/3	KA/3	KA/3	IV/1	IV/1	IV/2	IV/3	IV/5	IV/5	IV/5	IV/5	IV/5
SiO ₂	50.76	50.92	51.00	51.97	51.98	51.98	51.93	51.39	51.75	51.47	50.91	50.84	51.04	50.68	52.67	50.23	50.13	50.73	50.73	50.73	49.73
TiO ₂	1.13	0.97	0.93	0.79	0.62	0.62	0.65	0.67	0.63	0.88	0.86	0.81	0.50	0.80	0.46	1.07	1.01	0.32	0.32	0.32	0.19
Al ₂ O ₃	2.91	2.95	2.77	2.76	2.84	2.84	2.15	1.55	2.74	2.26	3.13	2.31	1.38	1.88	1.22	2.86	3.25	0.64	0.64	0.64	0.42
Cr ₂ O ₃	0.01	0.00	0.04	0.03	0.31	0.31	0.07	0.00	0.62	0.00	0.08	0.00	0.00	0.00	0.06	0.04	0.06	0.03	0.03	0.03	0.00
FeO	12.19	10.63	9.76	8.20	6.87	6.87	8.43	11.67	7.28	10.92	8.04	11.44	15.45	11.19	11.55	9.69	7.98	19.01	19.01	19.01	22.78
MnO	0.34	0.28	0.28	0.25	0.22	0.22	0.38	0.29	0.43	0.43	0.23	0.37	0.57	0.33	0.34	0.23	0.12	0.63	0.63	0.63	0.71
MgO	15.03	15.78	14.58	15.36	15.94	15.94	15.83	14.44	15.25	13.56	15.45	13.75	11.68	13.78	13.84	14.00	14.48	8.75	8.75	8.75	6.21
CaO	17.29	17.73	19.54	20.30	20.68	20.68	19.97	18.53	20.94	20.03	20.33	19.66	18.13	19.74	19.73	20.96	21.38	19.40	19.40	19.40	18.96
Na ₂ O	0.30	0.30	0.40	0.31	0.30	0.30	0.28	0.25	0.25	0.31	0.38	0.29	0.24	0.24	0.30	0.30	0.32	0.25	0.25	0.25	0.31
Total	99.95	99.56	99.30	99.97	99.76	99.76	99.58	98.88	99.75	99.86	99.41	99.47	98.99	98.64	99.42	99.38	98.73	99.76	99.76	99.76	99.31
Si	1.897	1.897	1.909	1.922	1.917	1.917	1.926	1.945	1.917	1.932	1.889	1.915	1.968	1.925	1.958	1.884	1.880	1.980	1.980	1.980	1.985
Ti	0.032	0.027	0.026	0.022	0.017	0.017	0.018	0.019	0.018	0.025	0.024	0.025	0.015	0.023	0.013	0.030	0.028	0.009	0.009	0.009	0.006
Al ^{IV}	0.103	0.103	0.091	0.078	0.083	0.083	0.074	0.055	0.083	0.068	0.111	0.085	0.032	0.075	0.042	0.116	0.120	0.020	0.020	0.020	0.015
Al ^{VI}	0.025	0.027	0.032	0.042	0.040	0.040	0.020	0.014	0.037	0.032	0.026	0.018	0.031	0.009	0.013	0.010	0.024	0.009	0.009	0.009	0.005
Cr	0.000	0.000	0.001	0.001	0.009	0.009	0.002	0.000	0.018	0.000	0.002	0.000	0.000	0.000	0.002	0.001	0.002	0.001	0.001	0.001	0.000
Fe ³⁺	0.037	0.043	0.034	0.013	0.021	0.021	0.036	0.020	0.011	0.009	0.063	0.042	0.003	0.037	0.023	0.065	0.060	0.010	0.010	0.010	0.022
Fe ²⁺	0.344	0.289	0.271	0.241	0.192	0.192	0.226	0.349	0.215	0.334	0.187	0.318	0.496	0.318	0.341	0.239	0.190	0.610	0.610	0.610	0.739
Mn	0.011	0.009	0.009	0.008	0.007	0.007	0.008	0.012	0.009	0.014	0.007	0.010	0.019	0.011	0.011	0.007	0.004	0.021	0.021	0.021	0.024
Mg	0.837	0.877	0.814	0.847	0.876	0.876	0.875	0.815	0.842	0.759	0.855	0.772	0.671	0.780	0.778	0.783	0.810	0.509	0.509	0.509	0.370
Ca	0.692	0.708	0.784	0.804	0.817	0.817	0.794	0.752	0.831	0.806	0.808	0.794	0.749	0.803	0.797	0.842	0.859	0.811	0.811	0.811	0.811
Na	0.022	0.022	0.029	0.022	0.021	0.021	0.020	0.018	0.018	0.023	0.027	0.021	0.018	0.018	0.022	0.022	0.023	0.019	0.019	0.019	0.024
Mg#	70.9	75.2	75.0	77.9	82.02	82.02	79.5	70.0	79.7	69.4	82.1	70.8	75.7	71.0	69.5	76.6	81.0	45.5	45.5	45.5	33.4
Al ^{VI} /Al ^{IV}	0.24	0.26	0.36	0.54	0.48	0.48	0.27	0.25	0.46	0.45	0.23	0.21	0.97	0.12	0.31	0.09	0.20	0.45	0.45	0.45	0.33
Wo	360	36.8	41.0	42.1	42.7	42.7	40.9	38.6	43.6	41.9	42.1	40.9	38.7	41.2	41.3	43.5	44.7	41.4	41.4	41.4	41.3
En	43.6	45.6	42.6	44.3	45.8	45.8	45.2	41.8	44.1	39.5	44.5	39.8	34.7	40.0	47.7	40.4	42.1	25.9	25.9	25.9	18.8
Fs	20.4	17.7	16.5	13.7	11.4	11.4	13.9	19.6	12.3	18.6	13.4	19.2	26.7	18.8	11.0	16.1	13.2	32.7	32.7	32.7	39.9

Formulae calculated on the basis of 4 cations and 6 oxygens. c = core, r = rim. Mg# = 100*(Mg/(Mg + Fe²⁺)). * = dacite. Sample location number corresponds to the locations in Figure 2A-B.

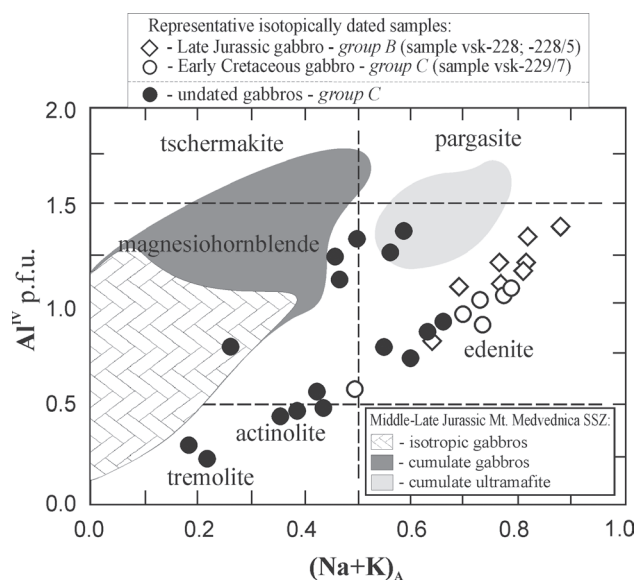


Figure 4: $Al^{IV} - (Na + K)_A$ plot of amphiboles from the Kalnik and Ivanščica Mts. gabbroic rocks with the nomenclature fields of LEAKE et al. (1997). Fields of amphiboles from the Mt. Medvednica Middle- to Late Jurassic gabbros and ultramafic cumulates (LUGOVIĆ et al., 2007; SLOVENEK & LUGOVIĆ, 2008) are shown for comparison.

Clinopyroxenes from the gabbroic group A, show the lowest Wo- and higher Fs-content (Fig. 5) and have significantly higher Ti-abundance than clinopyroxene populations hosted in the gabbroic rocks of groups B and C (Fig. 6; Table 2). The clinopyroxenes from group B show compositions similar to clinopyroxenes hosted in amphibole gabbros from

nearby Mt. Medvednica (Fig. 5) that are related to late Middle Jurassic intra-oceanic subduction in the ROD (SLOVENEK & LUGOVIĆ, 2008). In the same figure, the clinopyroxene populations from group A show a wide span of Fs-content and overlap with clinopyroxene compositions from rocks of group C.

6. BULK ROCK CHEMICAL COMPOSITION

Table 3 displays the results of 20 analyses of gabbroic rocks and 1 dacite from the Ivanščica and Kalnik Mts. tectono-sedimentary ophiolite mélangé. Nd and Sr isotopic composition of 6 gabbroic samples are shown in Table 4.

The analysed gabbroic rocks were subdivided on the basis of geochemical criteria into three geochemical groups (see Section 6 below) which were isotopically dated to three distinct geological times (see Section 7 below). The geochemical group A is represented by the Early Jurassic sample vsk-242/2 (Fig. 2A, location 1), group B by the Late Jurassic samples vsk-228 and 228/5 (Fig. 2A, location 4) and geochemical group C by Early Cretaceous samples vsk-229/7 (Fig. 2A, location 3) and sample vsi-8/1 (Fig. 2B, location 3).

The analysed gabbroic rocks partly underwent deuteric and sea-floor hydrothermal alteration which resulted in a minor increase in the loss on ignition ($LOI \leq 3.08$ wt%) and minor chemical modification of the major elements. In addition, the TiO_2 vs. Al_2O_3 diagram (COLOMBI, 1989) clearly shows that all analysed gabbros reflect basaltic liquid composition (Fig. 7A). This indicates that our gabbroic rocks may be considered to reflect original magmatic composition.

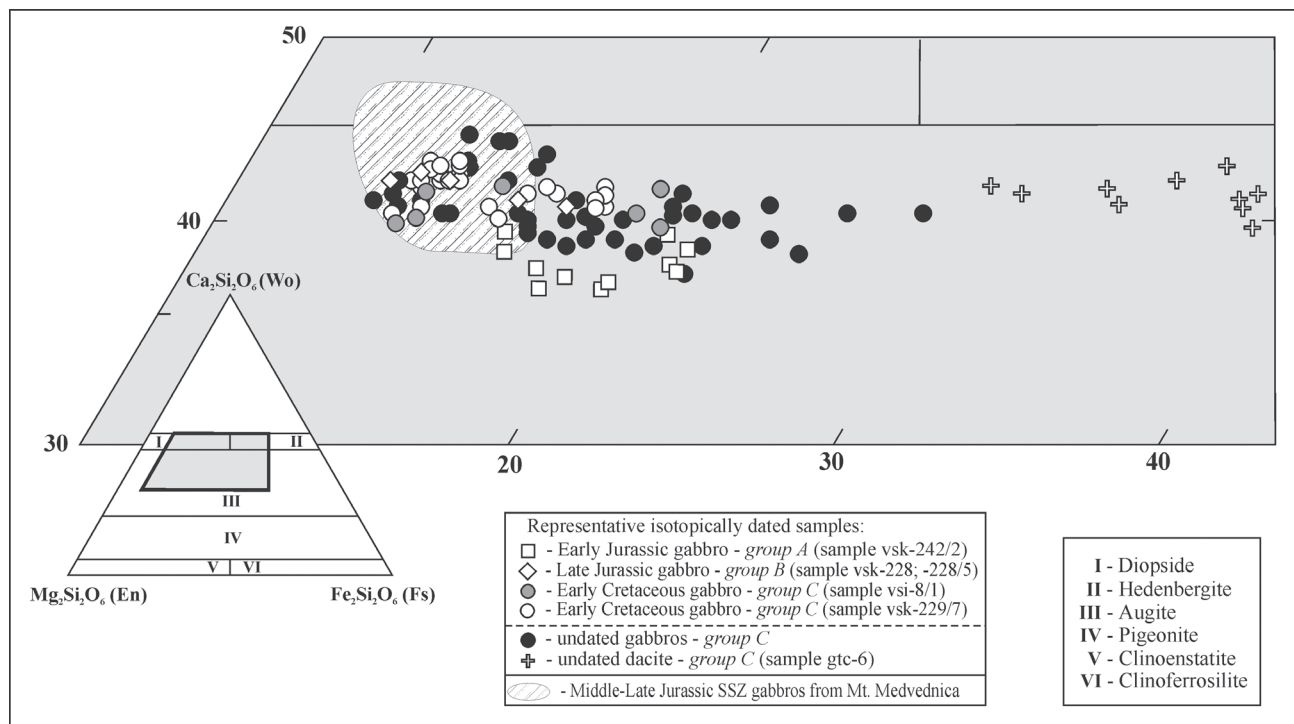


Figure 5: Plot of clinopyroxene compositions in the En - Wo - Fs ($Mg_2Si_2O_6 - Ca_2Si_2O_6 - Fe_2Si_2O_6$) diagram with the nomenclature fields of MORIMOTO (1988) for gabbroic rocks and dacite from the Kalnik and Ivanščica Mts. ophiolite mélangé. Field for clinopyroxene compositions from Middle- to Late Jurassic isotropic gabbros in the Mt. Medvednica ophiolite mélangé (SLOVENEK & LUGOVIĆ, 2008) are plotted for correlation constraints.

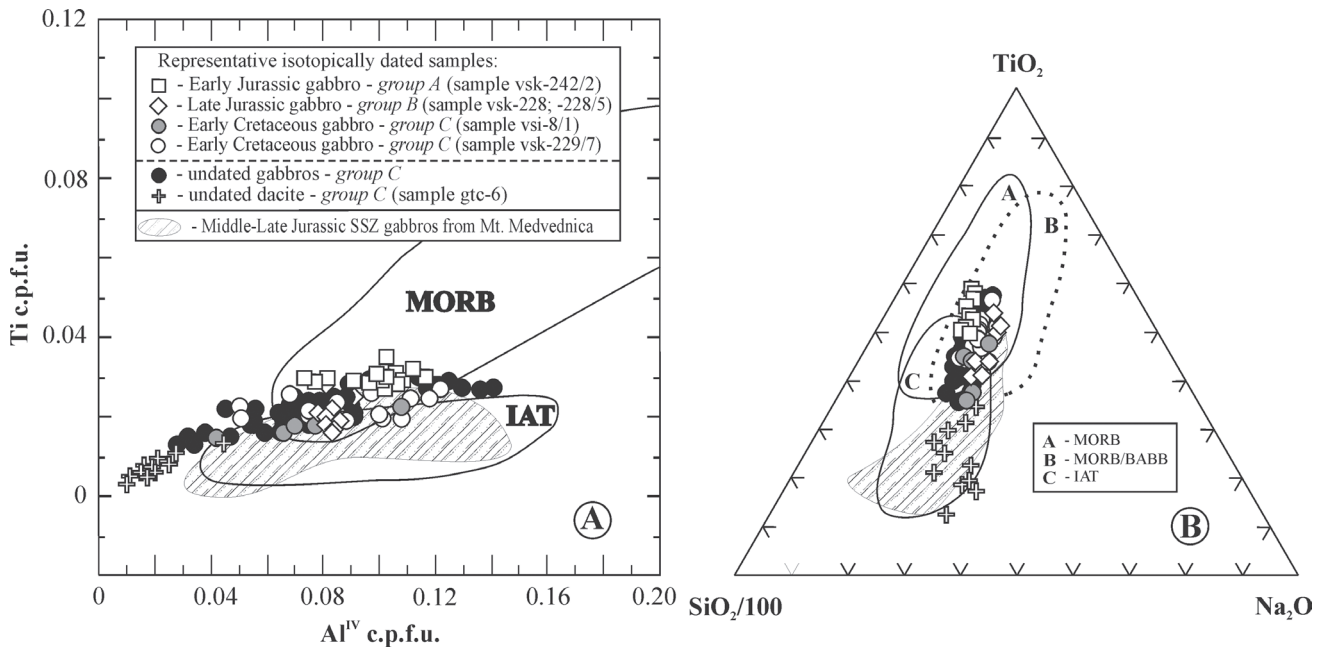


Figure 6: (A) Ti – Al^{IV} and (B) SiO₂/100 – Na₂O – TiO₂ discriminant diagram (simplified after BECCALUVA et al., 1989) for clinopyroxene from gabbroic rocks and dacite of the Kalnik and Ivanščica Mts. ophiolite mélangé. IAT = island-arc tholeiites, MORB = mid-ocean ridge basalts, BABB = back-arc basin basalts. Fields for clinopyroxene compositions from Middle- to Late Jurassic isotropic gabbros in the Mt. Medvednica ophiolite mélangé (SLOVENEC & LUGOVIĆ, 2008) are plotted for correlation constraints.

In the (Na₂O + K₂O) vs. SiO₂ classification diagram for intrusive rocks (COX et al., 1979), all rocks plot in the subalkaline field (Fig. 7B). The majority of the mafic samples plot in the gabbro field and only sample gtc-3 from Gotalovec quarry represents a true diorite composition, pointing to the relative immobility of Na and K. In the same type of diagram

for volcanic rocks, the felsic dyke (sample gtc-6) intersecting the Gotalovec quarry intrusives, plots in the dacite field (not shown). Samples from Gotalovec quarry represent the fractionated rocks, whereby sample gtc-4 is the least fractionated specimen. On the basis of co-variation of TiO₂ and Mg# following the classification scheme for ophiolitic gab-

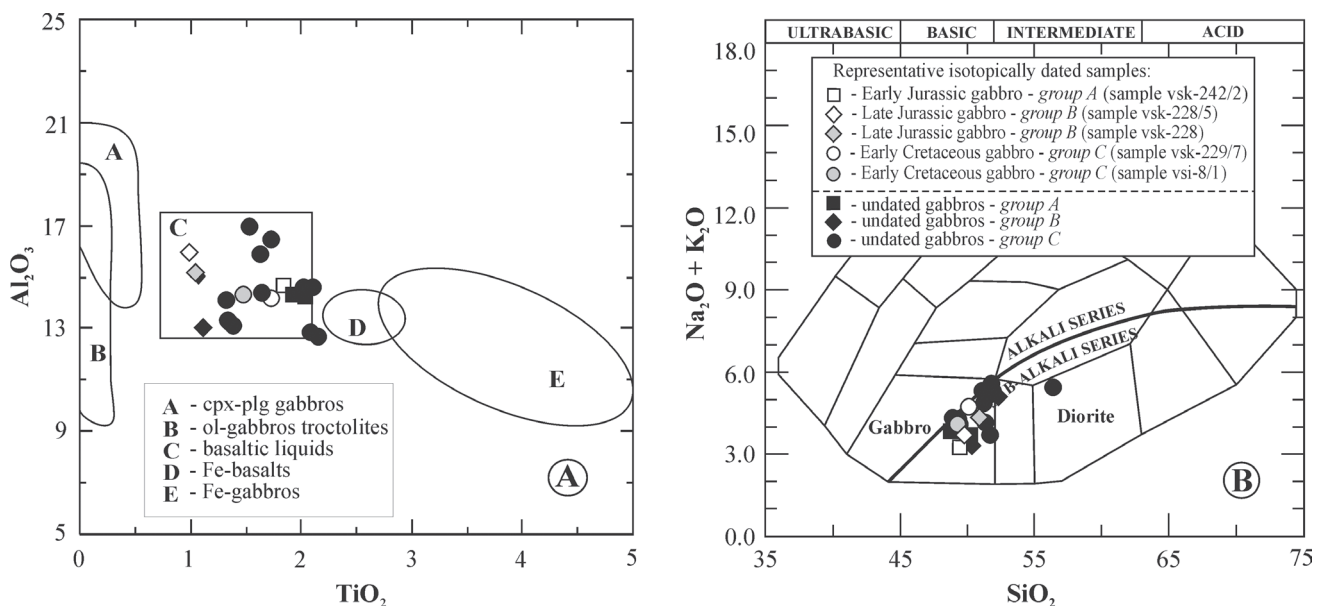


Figure 7: (A) Al₂O₃ – TiO₂ discrimination diagram (adopted from COLOMBI, 1989) and (B) TAS classification diagram with the nomenclature fields of intrusive rocks after COX et al. (1979) for the gabbroic rocks from the Kalnik and Ivanščica Mts. ophiolite mélangé.

Table 3: Chemical analyses of gabbroic rocks and dacite in the Kalmik (KA) and Ivanšćica (IV) Mts. ophiolite mélange.

Sample / Locality / Sample loc.	Group A			Group B					Group C										*gtc-6	
	vsk-242/2	vsk-242/4	vsk-242/6	vsk-228	vsk-228/2	vsk-228/5	vsk-217/1	vsk-229/1	vsk-229/7	vsk-229/12	be-3	vsi-5	vsi-7/1	vsi-8/1	vsi-8/2	gl-2	gl-5	+gtc-3		gtc-4
	KA/1	KA/1	KA/1	KA/4	KA/4	KA/4	KA/5	KA/3	KA/3	KA/3	IV/1	IV/2	IV/4	IV/3	IV/3	IV/5	IV/5	IV/5	IV/5	
SiO ₂	49.10	48.53	49.84	50.49	49.99	49.42	49.65	49.03	49.76	49.22	50.99	50.85	48.93	49.48	49.67	51.45	51.26	55.99	50.70	64.58
TiO ₂	2.06	2.25	2.14	0.97	0.99	0.91	1.35	1.66	1.74	1.50	2.13	2.29	2.19	1.36	1.35	1.64	1.55	2.04	1.74	0.51
Al ₂ O ₃	14.68	14.28	14.30	15.01	15.05	15.95	14.10	14.37	14.21	14.32	14.62	12.63	11.89	13.27	13.33	15.90	16.96	14.61	16.49	16.13
Fe ₂ O ₃ total	10.02	10.54	10.53	9.81	8.58	9.12	8.89	10.24	10.30	9.69	9.81	12.42	14.05	10.27	9.92	10.16	9.14	10.78	10.08	6.38
MnO	0.67	0.17	0.19	0.33	0.25	0.29	0.17	0.19	0.20	0.17	0.24	0.25	0.27	0.18	0.18	0.17	0.17	0.23	0.19	0.13
MgO	5.75	6.45	6.93	8.30	9.99	9.76	7.61	8.33	8.36	7.84	6.25	6.37	8.19	9.14	9.50	5.99	5.52	3.42	5.73	0.84
CaO	10.44	10.06	9.09	6.70	8.02	8.32	10.15	8.62	6.95	9.10	7.72	6.52	6.83	7.85	8.61	6.45	6.62	4.47	7.21	1.74
Na ₂ O	3.28	3.78	3.72	3.90	3.15	3.43	4.30	3.97	4.31	3.93	4.01	4.75	4.26	4.11	3.76	5.30	5.52	5.04	5.37	8.49
K ₂ O	0.04	0.08	0.05	0.49	0.19	0.47	0.03	0.18	0.80	0.37	0.19	0.16	0.08	0.24	0.01	0.07	0.01	0.47	0.02	0.23
P ₂ O ₅	0.22	0.23	0.20	0.08	0.09	0.07	0.17	0.16	0.18	0.15	0.28	0.21	0.23	0.15	0.12	0.18	0.23	0.36	0.17	0.10
LOI	3.05	2.95	3.05	2.62	3.03	2.26	3.08	3.06	2.75	2.93	3.05	3.04	2.07	3.01	3.03	2.99	2.92	3.04	0.24	1.61
Total	99.31	100.32	100.04	100.39	99.10	99.61	99.50	99.81	99.84	99.22	99.29	99.49	99.99	99.06	99.48	100.30	99.90	100.45	100.90	100.74
Mg#	53.24	56.08	57.84	68.99	71.30	67.61	62.90	62.25	62.34	63.59	58.20	50.79	54.88	64.41	67.91	54.25	55.15	40.38	56.07	23.04
Cs	0.2	0.1	0.1	1.2	1.4	0.8	1.0	2.6	3.8	2.3	1.6	1.0	0.2	0.3	0.6	2.0	0.2	1.2	1.3	0.8
Rb	1	1	2	15	15	16	1	8	7	11	8	13	3	2	3	1	1	11	1	5
Ba	54	79	67	314	208	355	78	164	341	172	608	657	74	188	174	114	75	237	47	125
Th	0.50	0.32	0.28	0.25	0.29	0.21	0.43	0.43	0.50	0.43	1.27	0.92	0.78	0.42	0.35	0.44	0.56	1.28	0.43	1.81
Ta	0.31	0.36	0.34	0.04	0.04	0.03	0.14	0.17	0.19	0.16	0.38	0.33	0.25	0.13	0.12	0.15	0.22	0.43	0.18	0.47
Nb	4.9	5.8	5.3	0.7	0.7	0.5	2.3	2.8	3.1	2.6	6.1	5.5	4.1	2.1	2.0	2.5	3.6	6.9	2.9	7.6
Sr	89	72	115	289	233	135	175	303	340	264	187	246	91	166	157	141	87	210	78	138
Zr	117	129	124	70	57	63	111	113	129	116	187	180	165	93	85	87	123	224	103	350
Hf	3.4	3.8	3.6	2.0	1.7	1.8	2.8	3.1	3.8	3.0	5.9	5.5	4.8	2.7	2.4	2.6	3.6	6.9	3.1	9.1
Y	39.7	42.5	43.1	27.6	25.0	27.2	34.2	33.4	35.8	33.7	58.7	58.5	51.4	32.4	29.8	30.3	45	75.9	35.4	90.7
Sc	41	40	37	42	38	36	37	40	37	38	27	37	38	40	42	35	28	22	35	11
V	333	380	346	338	357	321	289	318	318	300	328	411	375	279	279	319	285	322	305	273
Cr	110	125	130	260	252	244	200	290	250	160	19	19	20	400	450	40	30	18	34	20
Ni	40	39	41	<20	<20	<20	<20	<20	<20	<20	<20	<20	<20	60	40	40	30	30	31	<20
La	5.97	6.57	6.25	1.81	2.06	1.69	3.98	4.58	5.33	4.37	9.43	8.62	7.59	3.76	3.40	3.95	5.66	12.10	4.77	15.00
Ce	16.79	18.64	17.85	7.28	5.55	6.25	12.60	13.73	15.80	13.11	28.71	24.93	22.01	11.70	10.40	12.3	16.80	34.3	13.70	44.30
Pr	2.71	2.92	2.80	1.30	1.07	1.27	0.86	1.97	2.14	2.06	4.29	3.82	3.36	1.83	1.68	1.92	2.59	5.36	2.24	6.53
Nd	14.10	15.14	14.70	6.41	6.34	5.16	11.10	11.85	13.30	11.40	22.30	20.20	18.00	10.30	9.38	10.30	14.10	27.40	11.80	32.30
Sm	4.74	5.18	4.94	2.34	2.59	2.16	3.38	3.65	4.33	3.53	6.53	5.95	5.32	3.23	2.90	3.29	4.34	8.58	3.67	9.91
Eu	1.55	1.86	1.71	0.81	0.97	0.65	1.25	1.45	1.50	1.34	2.28	2.25	1.86	1.17	1.12	1.36	1.60	2.77	1.44	3.11
Gd	6.05	6.59	6.45	3.27	3.68	3.09	4.70	5.11	5.46	4.90	8.32	8.07	7.24	4.49	4.11	4.45	5.95	10.90	5.09	12.00
Tb	1.17	1.29	1.21	0.63	0.58	0.52	0.86	0.94	1.00	0.89	1.56	1.51	1.31	0.84	0.74	0.85	1.12	2.08	0.98	2.44
Dy	7.12	7.58	7.42	4.04	3.83	3.34	5.49	5.97	6.37	5.69	10.40	9.77	8.53	5.49	4.91	5.45	7.10	12.90	6.20	15.20
Ho	1.56	1.71	1.61	0.87	0.84	1.01	1.19	1.30	1.38	1.23	2.29	2.11	1.83	1.18	1.06	1.09	1.43	2.75	1.33	3.36
Er	4.59	4.81	4.09	2.78	2.85	2.37	3.63	3.95	4.23	3.69	6.99	6.40	5.60	3.58	3.24	3.27	4.31	8.03	3.82	10.10
Tm	0.672	0.701	0.683	0.433	0.396	0.445	0.514	0.558	0.598	0.525	1.001	0.905	0.796	0.504	0.448	0.478	0.626	1.191	0.557	1.610
Yb	4.48	4.74	4.54	3.08	2.92	3.11	3.31	3.51	3.84	3.42	6.46	5.90	5.20	3.18	2.92	3.13	4.13	7.71	3.62	10.10
Lu	0.682	0.718	0.701	0.442	0.402	0.455	0.483	0.509	0.570	0.493	0.926	0.884	0.760	0.468	0.430	0.463	0.632	1.250	0.573	1.620

Major elements in wt.%, trace elements in ppm. LOI = loss on ignition at 1100°C. Mg# = 100 * molar (MgO/(MgO+FeO_{total})). + = diorite, * = dacite. Sample location number corresponds to the locations in Figure 2A-B.

Table 4: Nd and Sr isotopic data of gabbros from the Kainik (KA) and Ivansčica (IV) Mts. ophiolite mélange.

Sample	Locality/ Sample loc.	Group	$^{147}\text{Sm}/^{144}\text{Nd}$	$^{143}\text{Nd}/^{144}\text{Nd}^a$	$^{87}\text{Rb}/^{86}\text{Sr}^a$	$^{87}\text{Sr}/^{86}\text{Sr}^a$	Sm	Nd	Rb	Sr	$\epsilon_{\text{Nd}(t)}^b$	$^{87}\text{Sr}/^{86}\text{Sr}_{(t)}^c$	Age (t)*
vsk-242/2	KA/1	A	0.20325	0.512923 (9)	0.032506	0.703208 (10)	4.74	14.10	1	89	+5.41	0.703122	185 Ma
vsk-228	KA/4	B	0.22072	0.512942 (8)	0.158975	0.704316 (9)	2.34	6.41	15	273	+5.47	0.703977	147 Ma
vsk-229/7	KA/3	C	0.19684	0.512923 (7)	0.059565	0.703762 (5)	4.33	13.30	7	340	+5.56	0.703673	105 Ma
vsk-229/12	KA/3	C	0.19549	0.512955 (3)	0.120551	0.703858 (4)	3.88	12.00	11	264	+6.20	0.703687	105 Ma
gi-2	IV/5	C	0.19313	0.512964 (15)	0.020518	0.703433 (14)	3.29	10.30	1	141	+6.43	0.703404	105 Ma
vsi-8/1	IV/2	C	0.18960	0.512950 (12)	0.034857	0.703564 (13)	3.23	10.30	2	166	+6.23	0.703514	105 Ma

Sample location number corresponds to the locations in Figure 2A-B. ^a Errors in brackets for Nd and Sr isotopic ratios are given at the 2 σ -level. The $^{147}\text{Sm}/^{144}\text{Nd}$ ratios calculated from Sm and Nd ICP-MS concentrations (displayed in ppm) following the equation: $^{147}\text{Sm}/^{144}\text{Nd} = (\text{Sm}/\text{Nd}) * [0.53151 + 0.14252 * ^{143}\text{Sm}/^{144}\text{Nd}]$. The $^{87}\text{Rb}/^{86}\text{Sr}$ ratios calculated from Rb and Sr ICP-MS concentrations (displayed in ppm) following the equation: $^{87}\text{Rb}/^{86}\text{Sr} = (\text{Rb}/\text{Sr}) * [2.6939 + 0.2832 * ^{87}\text{Sr}/^{86}\text{Sr}]$. ^b Initial $\epsilon_{\text{Nd}(t)}$ calculated assuming $t_{\text{CHUR}} = 0.512638$, $(^{147}\text{Sm}/^{144}\text{Nd})_{\text{CHUR}} = 0.1966$, and $\lambda_{\text{Sm}} = 6.54 * 10^{-12} \text{ a}^{-1}$. ^c Initial $^{87}\text{Sr}/^{86}\text{Sr}_{(t)}$ calculated assuming $\lambda_{\text{Rb}} = 1.42 * 10^{-11} \text{ a}^{-1}$. *Corresponding arbitrary age for the initial ϵ_{Nd} and initial Sr isotopic ratios.

Table 5: K–Ar ages of gabbroic rocks in the Kainik (KA) and Ivansčica (IV) Mts. ophiolite mélange.

Sample	Locality/ Sample loc.	Group	Analysed material	K [%]	40Ar (rad) nl/g	40Ar (air) [%]	Age Ma \pm 1 σ
vsk-228/5	KA/4	B	plagioclase	0.395	1.116	55.60	146.4 \pm 3.4
vsk-229/7	KA/3	C	plagioclase	0.709	3.067	68.41	107.6 \pm 4.2
vsi-8/1	IV/2	C	plagioclase	0.129	4.501	41.50	103.4 \pm 3.6

Sample location number corresponds to the locations in Figure 2A-B.

Table 6: $^{40}\text{Ar}/^{39}\text{Ar}$ data of amphibole from gabbro sample vsk-228 (geochemical group B) from the Mt. Kainik ophiolite mélange.

Step	Temp. (°C)	Time (min.)	$^{40}\text{Ar}/^{39}\text{Ar}$	$^{38}\text{Ar}/^{39}\text{Ar}$	$^{37}\text{Ar}/^{39}\text{Ar}$	$^{36}\text{Ar}/^{39}\text{Ar}$ $\times 10^{-2}$	Cum. ^{39}Ar (%)	Rad. ^{40}Ar (%)	Apparent age $\pm 1 \sigma$ s.d. (Ma)
1	600	10	5 \pm 18.0	0.68 \pm 0.09	19.9 \pm 1.70	252 \pm 23	1.59	0.67	58 \pm 204
2	700	10	30 \pm 6.0	0.41 \pm 0.07	12.2 \pm 0.50	188 \pm 8	4.48	5.50	316 \pm 65
3	800	10	-10 \pm 17.0	0.42 \pm 0.03	50.7 \pm 2.40	209 \pm 10	3.25	-1.67	-125 \pm 212
4	880	10	13.3 \pm 4.5	0.14 \pm 0.05	15.9 \pm 0.40	37 \pm 2	6.45	9.17	146 \pm 18
5	960	10	8.8 \pm 4.2	0.08 \pm 0.02	11.44 \pm 0.30	5 \pm 1	10.48	19.22	98 \pm 15
6	1040	10	14.0 \pm 2.0	0.15 \pm 0.11	17.27 \pm 0.35	2 \pm 1	18.58	37.69	153 \pm 11
7	1120	10	14.4 \pm 0.9	0.31 \pm 0.01	30.3 \pm 0.60	3 \pm 1	35.91	37.76	157 \pm 9
8	1200	10	22.4 \pm 1.2	0.21 \pm 0.01	30.1 \pm 0.60	23 \pm 1	19.26	17.44	239 \pm 12

Mass discrimination (measured $^{40}\text{Ar}/^{36}\text{Ar} = 279.9 \pm 0.2$), argon isotopic abundances corrected for line and furnace blank and nucleogenic interferences $^{40}\text{Ar}/^{39}\text{Ar}_K = 0.015 \pm 0.004$; $^{38}\text{Ar}/^{39}\text{Ar}_K = 0.018 \pm 0.002$; $^{36}\text{Ar}/^{37}\text{Ar}_{\text{Ca}} = 0.00043 \pm 0.00002$; $^{39}\text{Ar}/^{37}\text{Ar}_{\text{Ca}} = 0.00098 \pm 0.00003$). J-factor = 0.006321 \pm 0.000065 (BMus/2; t = 328.5 \pm 1.1 Ma, SCHWARZ & TRIEHOFF, 2007).

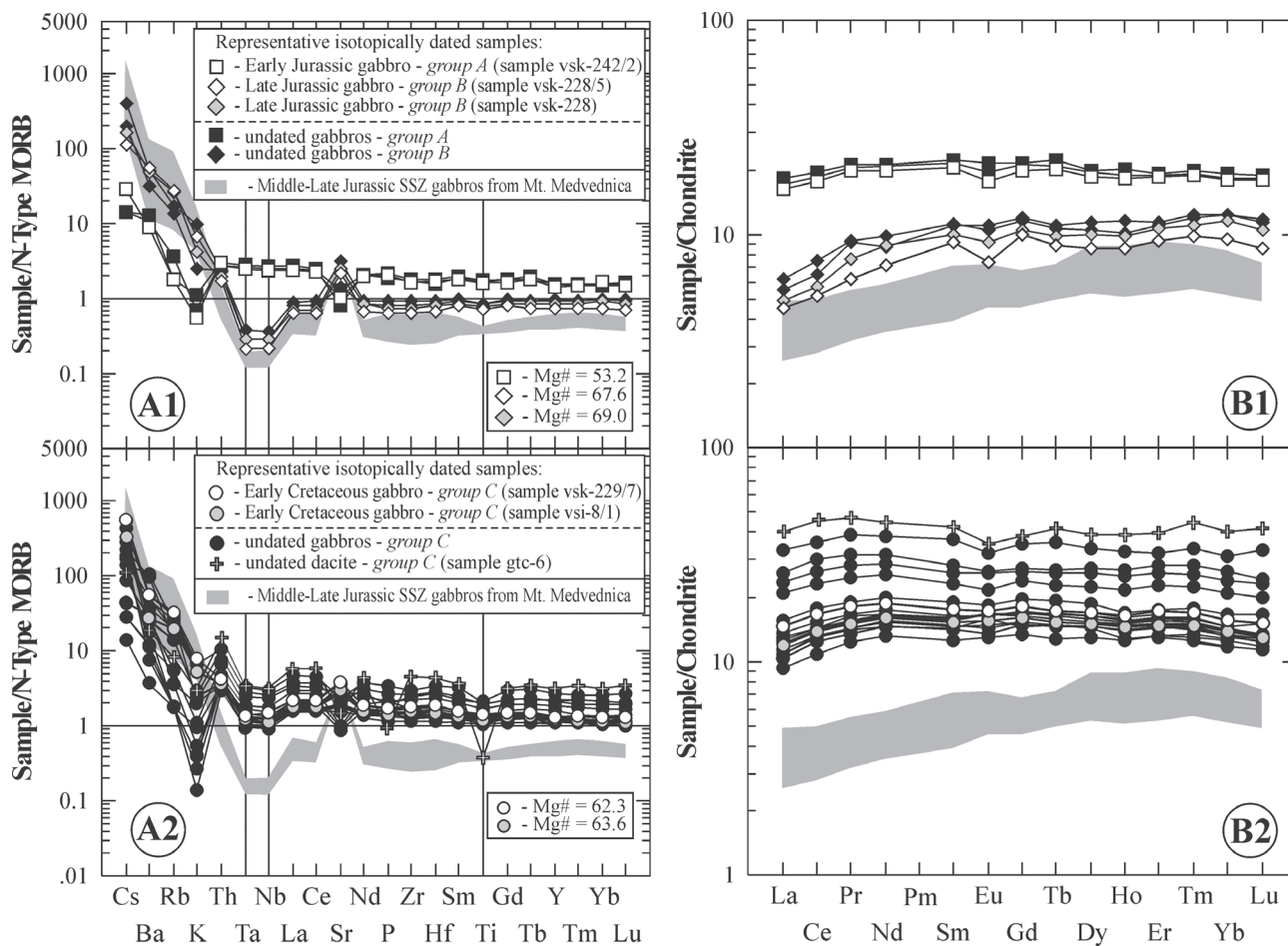


Figure 8: (A1, A2) N-MORB normalised multi-element diagram and (B1, B2) REE patterns for the Kalnik and Ivanščica Mts. gabbroic rocks and dacite. Normalisation values are from SUN and MCDONOUGH (1989). Patterns for Middle- to Late Jurassic isotopic gabbros in the Mt. Medvednica ophiolite mélange (SLOVENEK & LUGOVIĆ, 2008) are plotted for correlation constraints.

broic rocks (SERRI, 1981), the analysed samples of groups A and C correspond to a high-Ti gabbro (typical for a MORB/BABB setting) and samples of group B match to the low-Ti suite (typical for a SSZ setting).

Successive alteration may also mobilize trace elements that are very important indicators of petrogenetic processes and for the geotectonic formational setting of the rock. A test of trace element mobility in our samples was applied by plotting their concentration against Zr (not shown). High-field strength elements Ti, P, Ta, Nb, Y and Th (HFSE) as well as all rare earth elements (REE) appeared to be relatively immobile during alteration. In contrast, almost all large ion lithophile elements (LILE) showed selective, but generally high intensities of mobility and consequently will not be utilized for petrogenetic and geotectonic constraints. On multi-element abundance patterns normalized to N-type MORB, the analysed gabbros reveal a broad variety of compositions (Fig. 8A,B), suggesting different sources and/or fractional spans. Neglecting the LILE, which are selectively enriched due to alterations, the relative concentration profile is characterized by smooth patterns at 0.6 to 9.8 times relative to N-MORB. However, all samples of geochemical groups B and C display a negative anomaly for Nb, Ta and Ti, which is atypical for N-MORB, and indicates an input of a subduc-

tion component. These compositional patterns designated as N-MORB-type with arc signatures (SHERVAIS, 2001) are very common in mafic rocks of the Dinaric ophiolites (LUGOVIĆ et al., 1991; TRUBELJA et al., 1995). The absence of a subduction component input [$(\text{Nb/La})_n = 0.95-0.99$; $(\text{Ti/Gd})_n = 0.97-1.00$] is only observed in the gabbro samples of the group A that are generated during the Early Jurassic (Fig. 8A1). The highest input of subduction related components [$(\text{Nb/La})_n = 0.32-0.42$; $(\text{Ti/Gd})_n = 0.78-0.85$] is recorded in the Late Jurassic edenite gabbro samples of group B and suggests generation in an upper plate during intra-oceanic convergence. In these respects, they are very similar to the amphibole gabbros from the nearby Mt. Medvednica ophiolite mélange (Fig. 8A1). However, the Early Cretaceous gabbros of group C, show intermediate values [$(\text{Nb/La})_n = 0.58-0.69$; $(\text{Ti/Gd})_n = 0.74-1.07$; Fig. 8A2] between the gabbros of the former groups.

The analysed gabbros display similar chondrite normalized REE profiles at very different relative concentration levels which are characterized by flat patterns with a slight depletion in the LREE (Figs. 8B1 and 8B2). The intensity of LREE depletion expressed as $(\text{La/Sm})_{cn}$ increases from the representative Early Jurassic (group A) via the Early Cretaceous (group C) to the Late Jurassic (group B) gabbroic rocks

(0.79, 0.73-0.77 and 0.48-0.49, respectively). This is consistent with overall depletion of the samples shown by the concentration levels of their REE patterns (Figs. 8B1 and 8B2). The dacite dyke and host diorite from the Gotalovec quarry show MREE to HREE profiles 40-46 times relative to chondrite and represent highly fractionated compositions. The calculated range of Eu anomalies (0.77-1.09) is typical for fractionation and minor accumulation of plagioclase in the individual samples, respectively.

The measured $^{143}\text{Nd}/^{144}\text{Nd}$ ratios of gabbroic rocks are similar and vary from 0.512923 to 0.512964 which corresponds to respective initial $\epsilon_{\text{Nd}(T)}$ values ranging from +5.41 to +6.43 (Table 4). The $^{87}\text{Sr}/^{86}\text{Sr}$ ratios range from 0.703208 to 0.704316 and correspond to respective initial ratios of 0.703122 to 0.703977. The initial ϵ_{Nd} and $^{87}\text{Sr}/^{86}\text{Sr}$ ratios of the representative Early Jurassic (group A) gabbroic rock plot in the MORB field, while the all other representative Late Jurassic (group B) and Early Cretaceous (group C) gabbro samples plot in the field of recent island-arc and back-arc analogues (Fig. 9).

7. PREVIOUSLY PUBLISHED AND NEW ISOTOPIC DATING

7.1. K-Ar dating

Previously published K-Ar dating of the MORB-type gabbro south from of the Hruškovec quarry revealed an Early Jurassic (Pliensbachian) age of 185 ± 6 Ma (PAMIĆ, 1997). Here, a gabbro from the same block [sample vsk-242/2 (Fig. 2A, location 1)] is geochemically characterized and used as a representative for geochemical rock group A.

New K-Ar age data, presented here, are measured on plagioclase separated from gabbro [sample vsk-228/5 (Fig. 2A, location 4)] of geochemical rock group B, and two gabbros [sample vsk-229/7 (Fig. 2A, location 3) and vsi-8/1 (Fig. 2B, location 3)] of geochemical rock group C. The results are presented in Table 5.

We interpreted the ages as the ages of rock consolidation. The time of rock consolidation (146.4 ± 3.4 Ma) for gabbro which is used as a representative for geochemical rock group B in geological terms matches the Late Jurassic (Tithonian).

However, the other two ages (107.6 ± 4.2 Ma and 103.4 ± 3.6 Ma) obtained for BABB-type gabbros which are used as representatives for geochemical rock group C in geological terms correspond to the latest Early Cretaceous (Albian).

7.2. ^{40}Ar - ^{39}Ar dating

The results of the ^{40}Ar - ^{39}Ar measurements on a magmatic amphibole (edenite - Table 1, Fig. 4) separate of sample vsk-228 (Fig. 2A, location 4) are displayed in Table 6 and Figure 10. The initial heating steps indicate variable ages, steps 4-7 (with 70% of the released gas) suggest an apparent age of 147 ± 7 Ma. The last step of the spectrum is higher than the mean age, indicating inherited argon (e.g. from high-temperature minerals like apatite). The Ca/K spectrum (Fig. 10B) is increasing, suggesting some contamination of the mea-

sured sample by a mineral degassing at lower temperatures than amphibole and containing more potassium rather than calcium.

The plateau age of 147 ± 7 Ma from sample vsk-228 seems to be geologically significant, especially considering the similar age (146.4 ± 3.4 Ma) of sample vsk-228/5 from the same block obtained using K-Ar dating. We interpreted this plateau age as the age of gabbro crystallisation. Furthermore, it is (significantly) different in age from the gabbro south of the Hruškovec quarry of 185 ± 6 Ma. Therefore, this Late Jurassic gabbro is also used as a representative for geochemical rock group B.

8. DISCUSSION AND CONCLUSIONS

Besides the dominant extrusive oceanic rock fragments, the Kalnik Unit also contains blocks of deep crustal sequences represented by ultramafic cumulates (LUGOVIĆ et al., 2007), as well as mafic cumulate and isotropic plutonic rocks (SLOVENEK & LUGOVIĆ, 2008). The latter sequence, which was studied at the nearby Mt. Medvednica ophiolite mélange, comprises gabbro and predominant amphibole gabbro compositions, including a gabbro-pegmatite dated to 161.1 ± 2.1 Ma (Callovian-Oxfordian) (SLOVENEK & LUGOVIĆ, 2008). It was suggested that the Mt. Medvednica mafic-ultramafic crustal sequence represents remnants of a proto-arc-forearc system that was initiated in the ROD in Bathonian times (SLOVENEK et al., 2011). Isotropic gabbroic fragments are more abundant in the northern areas of the Kalnik Unit, in the Kalnik and Ivanščica Mts. ophiolite mélange. In this work, the analysed gabbroic rocks are subdivided on the basis of petrographic and geochemical criteria into three groups (group A, B and C) which were isotopically dated to three distinct geological times. These gabbroic rocks show a similar overall bulk rock chemistry (Fig. 8), isotopic compositions (Fig. 9) and clinopyroxene compositions (Fig. 5), that compare well with the analogues from the MORB, IAT and BABB geotectonic environments, respectively. This particularly holds true for the Early Jurassic and Early Cretaceous representative gabbros, whereas the Late Jurassic gabbros, follow an IAT trend also inferred for the Middle-Late Jurassic isotropic gabbros from the nearby Mt. Medvednica ophiolite mélange, as analysed by SLOVENEK & LUGOVIĆ (2008).

8.1. Tectonomagmatic and petrogenetic significance

a) Geochemical group A – Early Jurassic gabbroic suite

The amphibole-free gabbroic block [sample vsk-242/2 (Fig. 2A, location 1)], from Mt. Kalnik, dated by PAMIĆ (1997) to 185 ± 6 (Pliensbachian) has been assigned as the representative of the Early Jurassic geochemical group of rocks. Its geochemical characteristics are the most akin to slightly evolved N-MORB of all the analysed gabbro samples. This is evident from the normalized bulk rock chemistry (eg. multi-element abundance patterns normalized to N-type MORB; Fig. 8A1), initial Nd-Sr isotopic composition (Fig. 9) as well as the highest clinopyroxene Ti-abundances (Fig. 6) and position of the rocks in the selected geotectonic discrimination diagrams

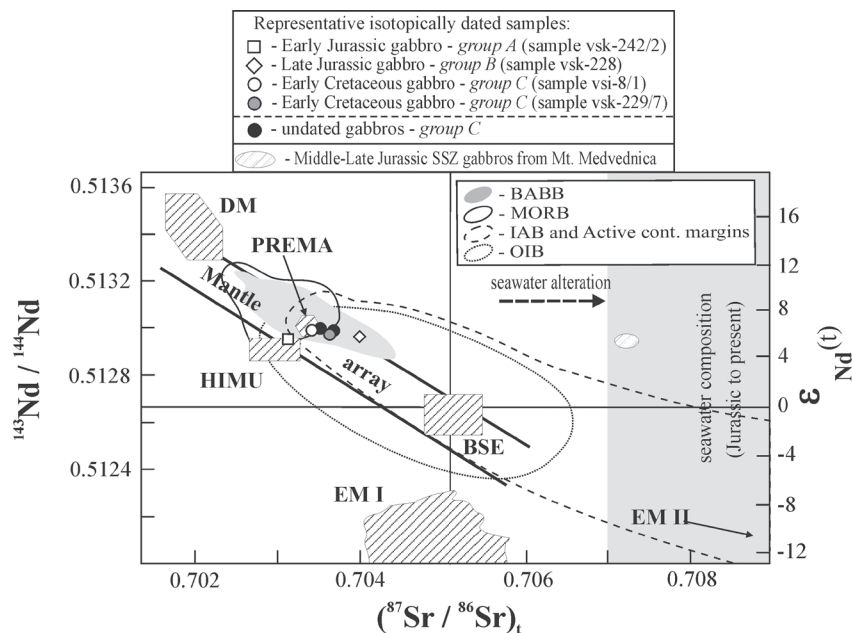


Figure 9: Initial $^{143}\text{Nd}/^{144}\text{Nd}$ – $^{87}\text{Sr}/^{86}\text{Sr}$ isotope ratios diagram for the Kalnik and Ivanščica Mts. gabbroic rocks showing the main oceanic mantle reservoirs of ZINDLER & HART (1986). Fields for Middle- to Late Jurassic isotropic gabbros in the Mt. Medvednica ophiolite mélangé (SLOVENEČ & LUGOVIĆ, 2008) are plotted for correlation constraints. DM – depleted mantle, BSE – bulk silicate Earth, EMI and EMI II – enriched mantle, HIMU – mantle with high U/Pb ratio, PREMA – PREvalent MAntle composition. The mantle array is defined by many oceanic basalts and a bulk Earth value for $^{87}\text{Sr}/^{86}\text{Sr}$ can be obtained from this trend. Data for back-arc basin basalts - BABB (shaded field) compiled from WILSON (1989) and references therein, COUSENS et al. (1994) and references therein, PEARCE et al. (1995), GRIBBLE et al. (1998) and EWART et al. (1998). Data for mid-ocean ridge basalts - MORB (solid line) compiled from WILSON (1989) and references therein and COUSENS et al. (1994), references therein and PEATE et al. (1997). Data for oceanic island arcs and active continental margins - IAB (broken line) compiled from WILSON (1989) and references therein, COUSENS et al. (1994) and references therein, PEARCE et al. (1995) and PEATE et al. (1997). The field for $^{87}\text{Sr}/^{86}\text{Sr}$ values affected by syn- or post-magmatic alteration in contact with seawater (light-grey shading) is from USTASZEWSKI et al. (2009).

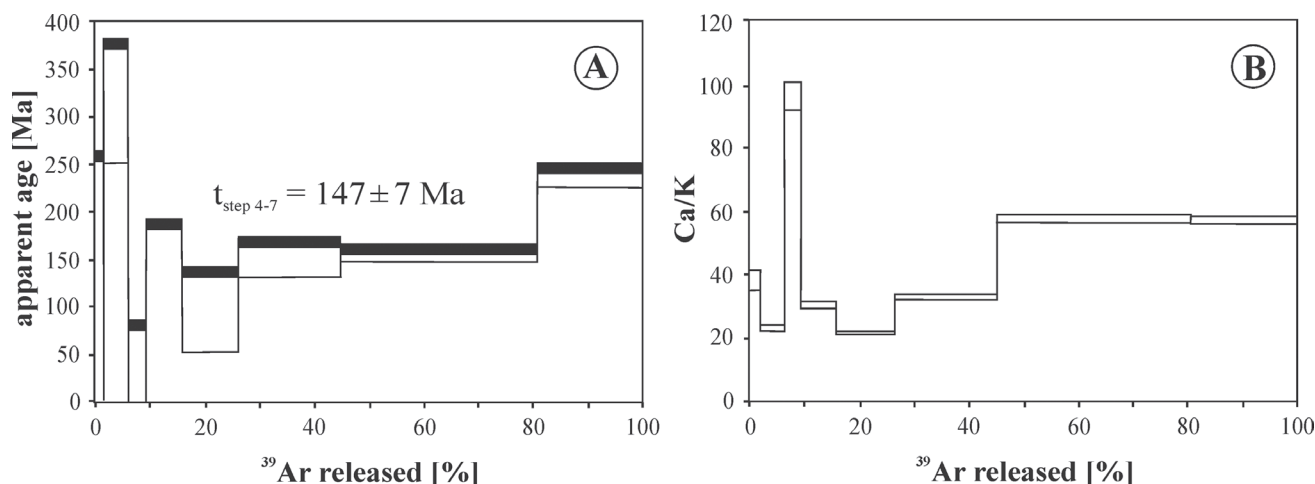


Figure 10: (A) $^{40}\text{Ar}/^{39}\text{Ar}$ step heating diagram of Late Jurassic gabbro amphibole (sample vsk-228) from the Mt. Kalnik ophiolite mélangé. (B) Ca/K spectrum.

(Fig. 11). The absence of the subduction component input expressed by the ratio $(\text{Nb}/\text{La})_n$ of 0.95-0.99, strongly suggests formation of the gabbroic rocks of group A at a ridge, spreading over a subducting slab at the terminal stage of the Palaeo-Tethyan slab break-off, which was previously dated to the Bajocian (SLOVENEČ et al., 2011). The amphibole-free gabbro represents a plutonic sequence of crust formed during the Early Jurassic onset of ocean-floor spreading in the ROD.

The residual mantle where these Early Jurassic gabbros were fractionated from should have extracted around 5% of partial melt (Fig. 12). However, a very high fertile mantle residuum (lherzolite) that is abundant in the CDOB ophiolite complexes (LUGOVIĆ et al., 1991; BAZYLEV et al., 2008) has not been previously observed in the ROD mélanges.

b) Geochemical group B – Late Jurassic gabbroic suite

A gabbroic crystallization sequence with magmatic amphibole, in this case edenite (Table 1, Fig. 4) represented in Late Jurassic samples vsk-228 and vsk-228/5 (Fig. 2A, location 4), in the context of ophiolites, is typical for the fractionation of tholeiitic basalts, under low to medium pressures in supra-subduction settings (SERRI & SAITTA, 1980). It is atypical for mafic rocks from an ocean ridge (PEARCE et al., 1984). However, accessory amphibole may crystallize at the ocean floor near to transform faults (CONSTANTIN, 1999) and mid-ocean ridges, where formation of Ti-pargasite-tschermakite is confined to the late-magmatic evolution of an intrusive sequence as an interstitial phase with low abundance (TRIBUZIO et al., 2000; COOGAN et al., 2001).

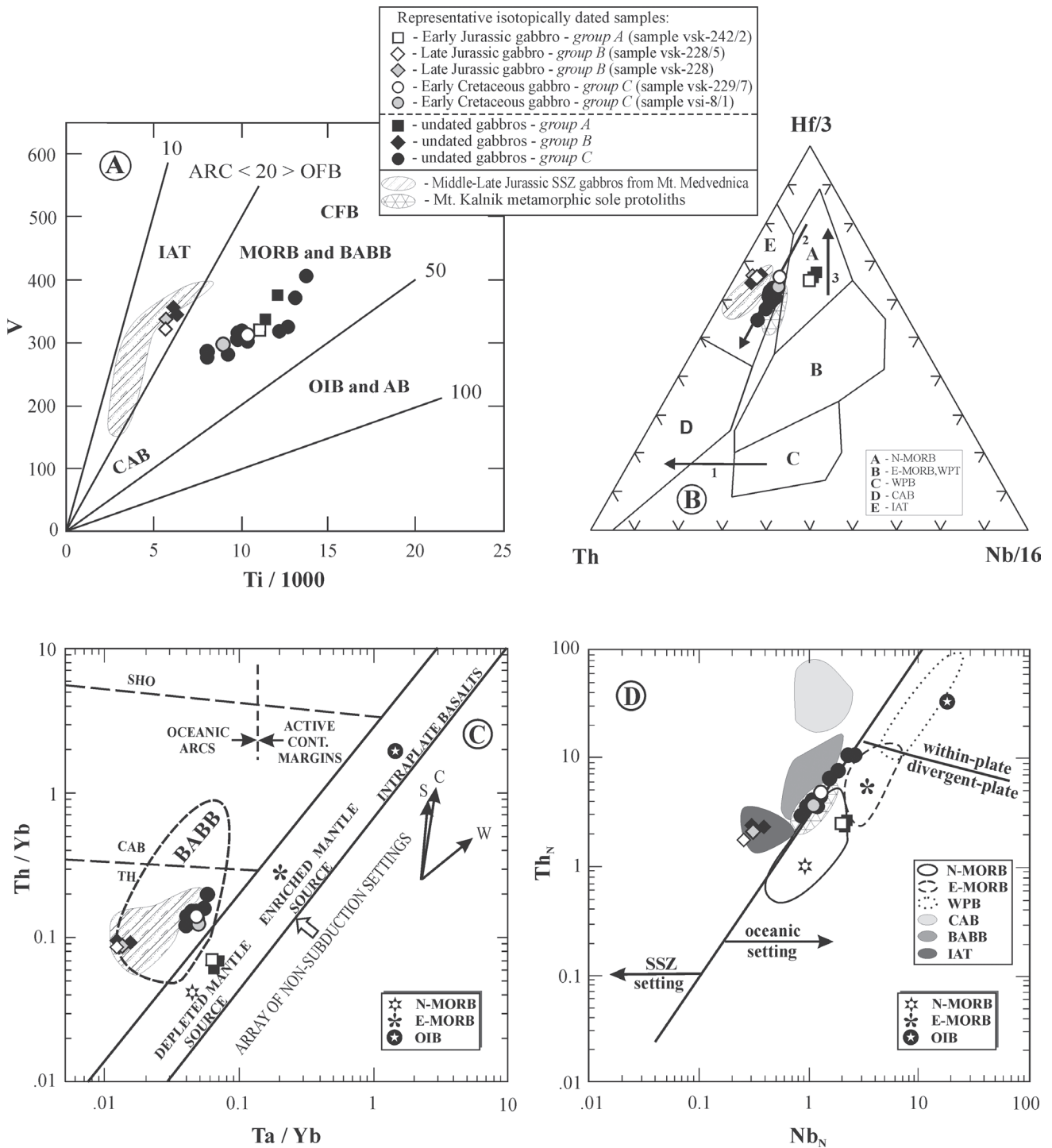


Figure 11: Discrimination diagrams for the gabbroic rocks from the Kalnik and Ivanščica Mts. ophiolite mélangé. (A) V – Ti/1000 diagram (SHERVAIS, 1982). IAT = island-arc tholeiites, MORB = mid-ocean ridge basalts, BABB = back-arc basin basalts, CAB = calc-alkaline basalts, CFB = continental flood basalts, OIB = ocean-island basalts and AB = alkali basalts. (B) Th – Hf/3 – Nb/16 diagram (WOOD, 1980). N-MORB = normal mid-ocean ridge basalts, E-MORB = enriched MORB, WPT = within plate tholeiites, WPB = alkaline within plate basalts, CAB = calc-alkaline basalts and IAT = island-arc tholeiites. 1 - crustal contamination; 2 - SSZ ophiolites trend; 3 - MORB ophiolites trend. (C) Ta/Yb – Th/Yb diagram (PEARCE, 1983). S - subduction zone enrichment; C - crustal contamination; W - within-plate enrichment. N-MORB, E-MORB and OIB are from SUN & MCDONOUGH (1989). T-MORB is from GESHI et al. (2007). Data for back-arc basin basalts (BABB) fields are from PEARCE et al. (1984), EWART et al. (1994) and LEAT et al. (2000). (D) Nb_N – Th_N diagram. Seven marked fields of different basaltic rock-type of Albanide-Hellenide ophiolites are from SACCANI et al. (2011). N-MORB, E-MORB and OIB are from SUN and MCDONOUGH (1989). T-MORB is from GESHI et al. (2007). Fields for Middle- to Late Jurassic isotropic gabbros in the Mt. Medvednica ophiolite mélangé (SLOVENEC & LUGOVIĆ, 2008) are plotted for correlation constraints.

In contrast, abundant magmatic amphibole is typical for rocks related to true subduction magmatism, sensu STERN (2004) that is, for the rocks crystallized from melt derived

from the mantle wedge, metasomatized by a flux of fluids released from the subducting slab. These volatile-rich magmas produced by hydrous melting of the mantle wedge (TATSUMI

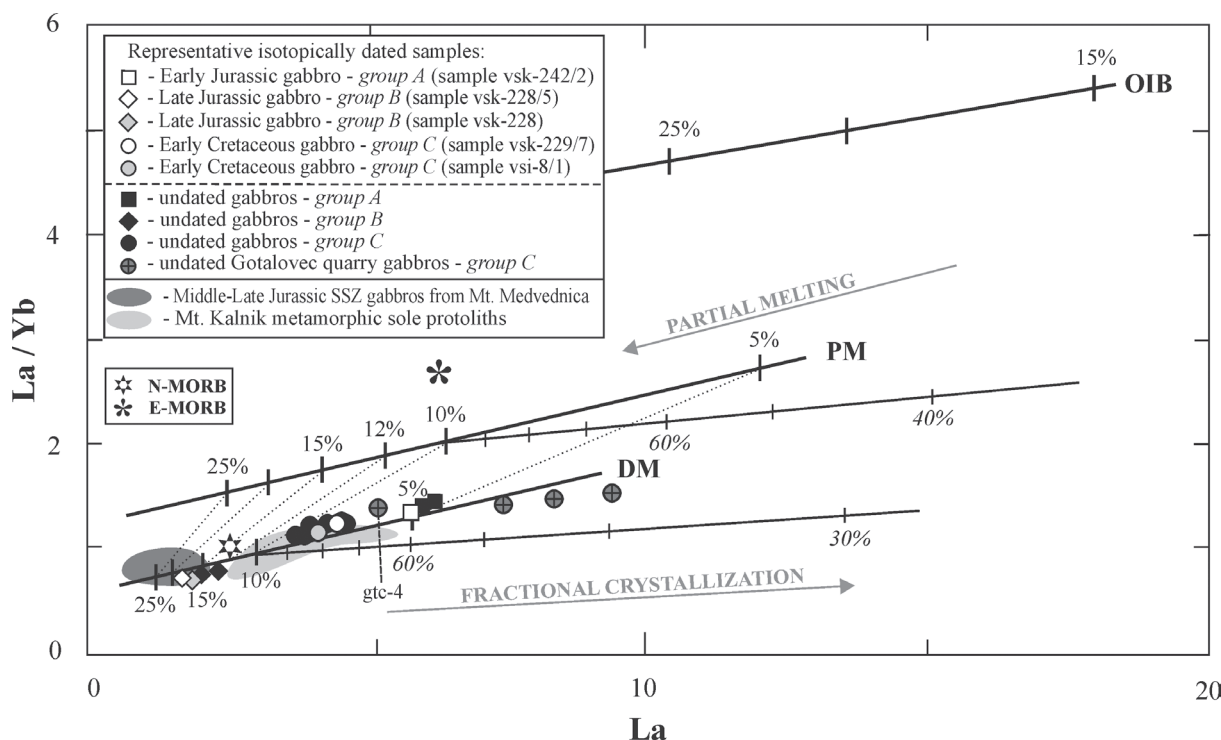


Figure 12: Petrogenic model for gabbroic rocks from the Kalnik and Ivanščica Mts. ophiolite mélange. Highly differentiated rock samples vsi-5 and vsi-7/1 from Mt. Ivanščica are omitted. Partial melting lines: DM – depleted mantle source, PM – primitive mantle source (KOSTOPOULOS & JAMES, 1992), OIB – enriched mantle source (CLAGUE & FREY, 1982). Model parameters = spinel-lherzolite source (ol₅₇-opx_{25.5}-cpx₁₅-sp_{2.5}), melting proportion = ol_{1.21}-opx_{8.06}-cpx_{76.37}-sp_{14.36}, distribution coefficients are from KOSTOPOULOS & JAMES (1992). Fractional crystallization lines: initial magma = 10% melting of DM and PM mantle source, respectively, fractionated mineral assemblage = ol₃₀-cpx₄₀-pl₃₀, distribution coefficients are from CHEN et al. (1990). Data for N-MORB, E-MORB are from SUN & MCDONOUGH (1989). Field for Middle- to Late Jurassic isotropic gabbros in the Mt. Medvednica ophiolite mélange (SLOVENEK & LUGOVIĆ, 2008) are plotted for correlation constraints.

& EGGINS, 1995) crystallize amphibole-bearing mafic-ultramafic rock associations, either in island-arcs or continental margins (CONRAD & KAY, 1984; DEBARI & COLEMAN, 1989; CLAESON & MEURER, 2004; KOCAK et al., 2005). Based on their strong mineralogical and geochemical similarities with recent or ancient lithological analogues, most of the blocks representing the oceanic plutonic succession archived in the Kalnik and Medvednica Mts. ophiolite mélange, must have formed in a supra-subduction setting. Samples vsk-204, vsk-228, vsk-228/2 and vsk-228/5 from Mt Kalnik (Fig. 2A, location 2 and 5), systematically plot in the field of island-arc tholeiites (Fig. 6 and 11). They show a strong subduction-related signature expressed as negative HFSE anomalies (Fig. 8A1). Initial ϵ_{Nd} and $^{87}Sr/^{86}Sr$ ratio (Fig. 9) also indicates their supra-subduction origin. At the same time, the sample shows significant depletion of LREE (Fig. 8B1), which is a peculiar geochemical feature of late Middle- to Late Jurassic supra-subduction magmatism, recorded by the extrusive blocks in the Kalnik and Ivanščica Mts. ophiolite mélange (SLOVENEK et al., 2011). The amphibole gabbros from the nearby Mt. Medvednica ophiolite mélange (Fig. 1A-B), although apparently older (~ 161 Ma; SLOVENEK & LUGOVIĆ, 2008), are more influenced by subduction related components (Fig. 6, 8 and 11). This suggests that the mantle wedge had been previously depleted in LREE by very small increments of melt removal, possibly similar to that for the mantle lherzolites in the CDOB, which are extremely depleted in LREE, particu-

larly in La (LUGOVIĆ et al., 1991; BAZYLEV et al., 2008). Subsequent subduction related enrichment of these peridotites in the mantle wedge will never increase La (as well as other LREE) concentration to an extent capable of producing a typical IAT REE pattern of partial melts (SLOVENEK & LUGOVIĆ, 2009). The Late Jurassic IAT-type amphibole gabbro is derived from the plutonic sequences of crust formed in the upper plate during initial subduction in the ROD. According to the La/Yb vs. La diagram (Fig. 12), the analyzed Late Jurassic gabbros from Mt. Kalnik, represent crust derived from a depleted mantle wedge that suffered around 13-17% partial melting. Amphibole-bearing transitional harzburgites inserted within the Campanian-Maastrichtian rudist limestones from Gornje Orešje in nearby Mt. Medvednica (LUGOVIĆ et al., 2007) with U-shaped REE patterns and slightly depleted spinel compositions (Mg# ~ 0.67; Cr# ~ 0.41) consistent with ~ 15% partial melting, perfectly matches the residual mantle after extraction of the parental melt. Another transitional harzburgite slice from Gornje Orešje showing a more depleted spinel composition (Mg# ~ 0.56; Cr# ~ 0.45) which is consistent with ~ 20% partial melting, may represent vestiges of the residual mantle from where the Mt. Medvednica gabbros were derived.

The geochemical signatures of the gabbro samples vsk-228 and vsk-228/5 indicate magmatism at around ~ 147 Ma (Tithonian) related to a nascent island-arc setting. Since this age is younger than those obtained on island-arc basalt from

Ivanščica Mt. (154 ± 8.7 Ma; see SLOVENEČ et al., 2011), this is the youngest measured age concerning the Late Jurassic intra-oceanic subduction related crust in the ROD.

c) Geochemical group C – Early Cretaceous gabbroic suite

The gabbroic blocks represented by samples vsk-229/7 from Mt. Kalnik and vsi-8/1 from Mt. Ivanščica, dated to the latest Early Cretaceous (Albian) have been adopted as the representative samples of group C. This group also includes undated isotropic gabbro samples with the same or very similar geochemical and mineralogical compositions and characteristics (Table 1-3, Fig. 4-9 and 11). Gabbros from this block contain minor amounts of edenite (Table 1; Fig. 4), suggesting crystallization from a volatile-bearing magma. Given the bulk rock chemistry, (Table 3; Fig. 8) and host clinopyroxene composition (Table 2; Fig. 6), the gabbros show transitional geochemical signatures between the Early Jurassic N-MORB-type gabbros of group A and the Late Jurassic IAT-type gabbros of group B. Geochemical features compiled from selected discrimination diagrams (Fig. 11) as well as initial ϵ_{Nd} and $^{87}Sr/^{86}Sr$ ratios (Fig. 9) indicate the BABB-type affinity of this gabbroic group that clearly forms a discrete trend (Fig. 11B and 11D). This suggests that the rock suite of group C may represent cogenetic crustal fragments derived from a similar mantle source. These Early Cretaceous gabbros are formed in an ensimatic back-arc marginal basin of the ROD. Since those gabbros reflect basaltic liquids (Fig. 7A), their compositions may be used for petrogenetic modelling. The representative gabbro samples and other members of the group, except Gotalovec quarry samples, show ~ 7-9% total partial melting (Fig. 12). However, the Gotalovec quarry sample gtc-4, albeit being slightly fractionated, may reflect melts derived from a comparatively slightly more depleted mantle source. The other three Gotalovec quarry gabbros are moderately fractionated (Fig. 12). The highly serpentinized lherzolite from the Mt. Kalnik metamorphic sole, that has undergone 7% of partial melting (LUGOVIĆ et al., 2007), perhaps could be compositionally reminiscent of the mantle residue of these representative gabbros. The Kalnik lherzolite is LREE depleted due to very small increments of melt removal and in this respect closely resembles Jurassic mantle lherzolites from the CDOB ophiolite complexes (LUGOVIĆ et al., 1991; BAZYLEV et al., 2008).

The existence of Early Cretaceous oceanic crust in the ROD may be inferred from protoliths of the almandine amphibolite facies metamorphic sole, welded beneath the Mt. Kalnik lherzolite (LUGOVIĆ et al., 2007). The metamorphic sole includes BABB-type protoliths from plutonic and extrusive sequences that were metamorphosed at 118 ± 8 Ma (IGNJATIĆ, 2007). The formation of a metamorphic sole bears witness to the termination of spreading and indicates the initial stages of convergence in an oceanic basin, wherein the youngest oceanic crust and parental mantle are involved in a contact dynamo-thermal interaction (e.g. INSERGUEIX-FILIPPI et al., 2000; WAKABAYASHI & DILEK, 2000, 2003). The amphibolite-lherzolite composite slice from Mt. Kalnik is tectonically emplaced into Palaeocene carbonate breccias and represents the remnant that provides the crucial

key to understanding the tectonomagmatic evolution in the final oceanic stage of the ROD.

Unfractionated and least fractionated samples of group C from Figure 12 resemble the geochemical characteristics of the Aptian metamorphic sole protoliths (Fig. 11B and 11D), and may be interpreted as crust formed in an Early Cretaceous back-arc basin. Alternatively, a similar rock suite may have formed during the subduction of an active ridge (e.g. BORTOLLOTTI et al., 2002), when an enormous volume of magma generated in a relatively short period of time, creates incipient crust in the leading edge of the upper (overriding) plate (e.g. STERN & BLOOMER, 1992). From this standpoint, the same rock suite should be relatively younger than in the model that assumes its formation at a back arc basin spreading ridge. However, a full time range of crust formation in the Cretaceous back-arc basin of the ROD requires extensive dating.

The composite gabbroic megablock from the Gotalovec quarry (Fig. 2B, location 5) shows a high level of magma fractionation resulting in minor diorite, and finally in the intersecting tholeiitic dacite. These petrogenetic characteristics of the rocks reflect pressure release melting, fractionation and formation of felsic compositions which is analogous with crust formation during the early stage of widening in the modern back-arc basin (SINTON et al., 2003). Continuous normal zoning observed in edenite suggests fractional crystallization in a closed, deep-seated magma system (STERN, 1979). The edenite Al- and Ti-content thermobarometer (ERNST & LIU, 1998) suggests the crystallization pressures and temperatures for the Gotalovec megablock were 0.6 GPa at 860 °C. Their petrological characteristics suggest formation at a slow-rate spreading ridge of a marginal basin. However, the alteration pattern of the Gotalovec quarry gabbroic plutonic rocks is, according to the evidence, in many ways similar to that of accreted island-arc terrains reported by MAHLBURG & KAY (1983), particularly concerning exsolved Mn-rich ilmenite. Assuming the type of alterations atypical for ridge crust, Gotalovec quarry deep crustal rocks must have acted as the leading edge of a back-arc upper plate.

The Cretaceous back-arc basin mantle from the ROD is comparable in most mineralogical and geochemical features to mantle peridotites from the Early Jurassic CDOB ophiolites. This may suggest that it was not affected by the subduction that commenced in the ROD in the Middle Jurassic (Bathonian). If these assumptions concerning gabbroic rocks are generally correct, then rifting and formation of the back-arc spreading centre must have initiated in the Early Jurassic (or older ?) lithosphere behind the island-arc. The mode of back-arc opening in the ROD is apparently different to that proposed for most modern back-arc basins (see MARTINEZ et al., 2007).

8.2. Improved geodynamic model for the ROD

In geotectonic modelling of the Neo-Tethyan realm, the ROD ophiolites belong to its easternmost segment (BORTOLLOTTI & PRINCIPI, 2005). Disagreement exists as to whether the fragmented ROD oceanic lithosphere, including lithosphere related to the advanced stage rifting has a Di-

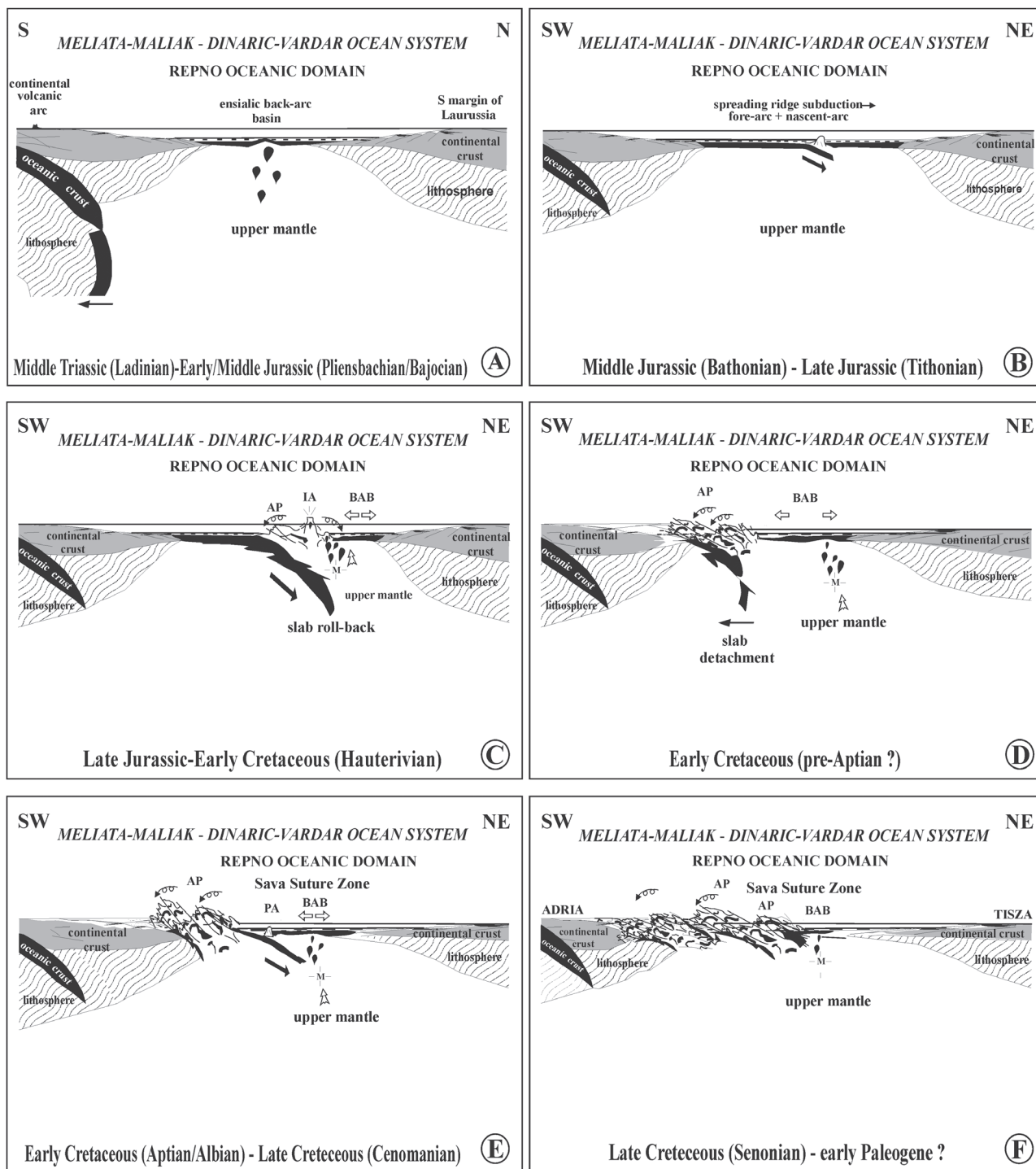


Figure 13: Improved schematic geodynamic model for the evolution the Repno oceanic domain as a corner domain connecting the Meliata-Maliak and Dinaric-Vardar oceanic systems. (A) The first spreading stage and formation of ensialic back-arc basin. (B) The early stage of the first subduction in the ROD with formation of an infant proto-arc. (C) The evolved subduction stage with initiation of an island arc and formation of the subsequent ensimatic marginal (back-arc) basin. (D) Ongoing spreading in the back-arc basin – the second spreading stage in the ROD. (E) Subduction in the back-arc basin – the second subduction stage in the ROD with the formation of a proto-arc (?) in the overriding plate. (F) The closure stage of the ROD. 1 – mantle diapir, 2 – oceanic crust with radiolarian cherts, 3 – raising of the mantle diapir, 4 – melting zone; AP = accretionary prism BAB = back-arc basin, PA = Cretaceous proto-arc.

naric-Vardar oceanic provenance (e.g. PAMIĆ, 1997; HAAS & KOVÁCS, 2001; KISS et al., 2012), or is a segment of the Meliata-Maliak oceanic system (e.g. GORIČAN et al.,

2005; SLOVENEK & LUGOVIĆ, 2008, 2009; SLOVENEK et al., 2010, 2011). However, the ROD indeed represents a corner stone domain between these two oceanic systems

(Fig. 1C), which for example after BABIĆ et al., (2002) and SCHMID et al. (2008), are assumed to be integral parts of one and the same ocean basin. In general, all parts of the oceanic domain shared a common tectonomagmatic evolution throughout the Mesozoic, although some events might be locally specific and diachronous.

The data presented here chronologically defines the late stage of Early Jurassic spreading, a nascent stage of island-arc formation in the Late Jurassic, and may suggest the existence of a Cretaceous back-arc marginal basin from the Sava-Vardar Suture Zone (PAMIĆ, 2002) or, in other words, from the inner part of the Western Vardar Ophiolite Unit (SCHMID et al., 2008). Therefore, the results presented in this work only complement the previously proposed segmental model of the geodynamic evolution of the ROD. The proposed model of the geodynamic evolution of the ROD presented in this paper represents a comprehensive model based on all the up to date published research results (see SLOVENEK & LUGOVIĆ 2009, 2012; SLOVENEK et al., 2010, 2011).

In the framework of the Dinaric-Vardar oceanic provenance, the ROD probably commenced its geodynamic evolution as an ensialic back-arc basin formed behind a peri-continental volcanic arc, related to Andean-type subduction of the Palaeo-Tethyan lithosphere beneath the European continental margin (STAMPFLI & BOREL, 2002, 2004; GORIČAN et al., 2005). Alternatively, it may have formed as a westward prograding embayment of the Neo-Tethys Ocean (see discussion in PAMIĆ et al., 2002; ROBERTSON et al., 2009).

The oldest record of rifting of the intra-continental lithosphere behind the peri-continental volcanic arc was dated as late Anisian, specifically as Illyrian (SLOVENEK et al., 2010). The advanced stage rifting is characterized by pelagic carbonate peperites (HALAMIĆ et al., 1998; PALINKAŠ et al., 2000, 2008). The onset of rifting created a rift basin with pelagic sediments and within plate alkali basalt - type crust (SLOVENEK et al., 2010, 2011; KISS et al., 2012). This basin was located between the future Adriatic microplate and the continental edge of south Laurussia (represented by pieces of the recent ALCAPA, Dacia and Tisza Mega-Unit; Fig. 1A-B), at least in the early Ladinian. The oldest spreading ridge oceanic crust related to the proto-oceanic stage (first spreading stage in the ROD) is represented by enriched E-MORB-type extrusive rocks formed in the early Ladinian, particularly the late Fassanian, and was followed by depleted E-MORB-type crust in the late Ladinian, T-MORB-type crust in the middle Carnian and the first appearance of N-MORB-type crust in the late Carnian (SLOVENEK et al., 2011; Fig. 13A). Such a regular chemostratigraphic succession of ridge crust formation through the opening of an ocean reflects a slow spreading rate (eg. WILSON, 1989).

The T-MORB-type and N-MORB-type crust formed during spreading from the middle to late Carnian, displays slight supra-subduction characteristics inherited from the Middle Triassic subduction of the Palaeo-Tethys (or an earlier subduction?). The inherited SSZ characteristics systematically diminished through the onset of spreading after the late Carnian and completely disappeared until the Bajocian

oceanic crust due to the subducting slab-break-off (SLOVENEK & LUGOVIĆ, 2009). Therefore the Bajocian crust is assumed to represent the maximum evolved stage of spreading in the ROD (SLOVENEK & LUGOVIĆ, 2012). However, this work suggests that the sinking slab should have already broken-off in the Pliensbachian (Fig. 13A).

Intra-oceanic convergence (the first stage of subduction in the ROD) commenced in the late Middle Jurassic (late Bathonian) as recorded by subduction of an active oceanic ridge and production of “N-MORB with arc signature” crust in the overriding plate (SLOVENEK & LUGOVIĆ, 2009; Fig. 13B). At this stage magmatism was not related to a significantly metasomatized mantle wedge (sensu STERN (2004) and WHATAM & STERN (2011)), and does not represent true subduction derived igneous activity. Due to the onset of spreading accompanied by progressive metasomatism of the mantle wedge during the Callovian-Oxfordian, the IAT-type crust was produced in an infant proto-arc extensional setting (SLOVENEK et al., 2011; Fig. 13B). The youngest IAT-type edenite gabbro dated here as Tithonian represents the youngest crust related to the first subduction event in the ROD that reflects the nascent stage of formation of an intra-oceanic volcanic arc. Although the amphibole-bearing gabbroic rocks from the nearby Mt. Medvednica ophiolite mélange (SLOVENEK & LUGOVIĆ, 2008) are more influenced by subduction related components, they show older formational ages (~ 161 Ma vs. ~ 147 Ma). This inverse chemostratigraphic evolution suggests that true SSZ magmatism might have been delayed and/or was diachronous during the onset of the first subduction event in the ROD. Moreover, it indicates specific metasomatically induced thermal regimes of hydrous partial melting along the subduction front (Fig. 13C).

A modern fore-arc progressed over a period of about 15 Ma to a mature island arc, accompanied by a coeval and cognate back-arc basin (STERN et al., 1996; BLOOMER et al., 1995). Rocks typical for a mature island-arc, such as calc-alkaline extrusives, have not yet been reported for the ROD and represent a missing link needed to complete the geodynamic model.

The back-arc marginal basin in the ROD must have formed during the Early Cretaceous, but it is not clear when the spreading (second spreading stage in the ROD) commenced (Fig. 13D). The Early Cretaceous BABB-type lower crust and related mantle peridotites from the ROD show evidence against island-arc involvement in the rifting. Therefore the rifting must have initiated behind the island-arc and led to formation of the extensional back-arc basin. The metamorphic sole derived from BABB-type crust dated to 118 ± 8 Ma (IGNJATIĆ, 2007) indicates termination of back-arc spreading in the basin during the Aptian. Simultaneously, a thick island-arc crust was emplaced onto the continental margin of the Adriatic plate, forming the Mt. Medvednica lower greenschist facies metamorphic complex, and consists of rocks of both pericontinental and oceanic provenance (LUGOVIĆ et al., 2006, with references). Since the greenschists derived from IAT-protoliths dated to 119 ± 5 Ma (BELAK et al., 1995), the formation of the metamorphic sole in

the back-arc basin, and the emplacement of the island-arc onto the Adriatic continental margin, did not appear as sequential events. Formation of oceanic crust in the ROD must have continued after the Aptian, and obviously in the upper plate (second subduction stage in the ROD; Fig. 13E). This is indicated by the youngest Early Cretaceous (Albian) ophiolites back-arc affinity of rock group C. The back-arc basins or marginal basins located in front of the Tisza-Dacia Mega-Units, where the oceanic crust was formed during the latest Early Cretaceous to early Campanian (e.g. USTASZEWSKI et al., 2009 with references therein), (referred to as ophiolites of rock group C), are included in the Sava-Vardar Zone (PAMIĆ, 2002; Fig. 1A), or simply the Sava Zone (SCHMID et al., 2008). This Sava-Vardar zone is thought to be a suture zone between the Dinarides and fragments of the European continental margin (Fig. 1A). Following this model, the ROD back-arc basin from the Aptian (formation of metamorphic sole) onwards, may be interpreted as one of several discrete marginal basins stretching along the Sava-Vardar-Izmir-Ankara-Erzincan Suture Zone. The next Cretaceous marginal basin domain of this suture zone may be envisaged in North Kozara in the southeast (Fig. 1A) where Campanian bimodal magmatic succession reflects its stage of closure (USTASZEWSKI et al., 2009; model b2).

The ROD back-arc basin closed to a great extent during the latest Late Cretaceous (Fig. 13F) as deduced from peridotite clasts in Campanian basal conglomerates (HALAMIĆ, 1998), subaerial weathering of peridotites into Ni-lateritic crust (PALINKAŠ et al., 2006) and composite peridotite-amphibolite slices tectonically emplaced into Palaeocene breccias (LUGOVIĆ et al. 2007).

ACKNOWLEDGEMENT

This work is the contribution to the scientific projects: Mesozoic magmatic, mantle and pyroclastic rocks of northwestern Croatia (grant no. 181-1951126-1141 to Da. S.) and Tectonomagmatic correlation of fragmented oceanic lithosphere in the Dinarides (grant no. 195-1951126-3205 to B. L.), carried out under the support of the Croatian Ministry of Science, Education and Sport. Critical comments by Vesnica GARAŠIĆ and an Anonymous Reviewer greatly helped to achieve final version of the manuscript.

REFERENCES

- BABIĆ, L.J., HOCHULL, P.A. & ZUPANIĆ, J. (2002): The Jurassic ophiolitic mélange in the NE Dinarides: Dating, internal structure and geotectonic implications.– *Eclogae Geologicae Helveticae*, 95, 263–257.
- BALEN, D., SCHUSTER, R. & GARAŠIĆ, V. (2003): The Kamenjača olivine gabbro from Moslavačka Gora (South Tisia, Croatia).– *Rad Hrvatske akademije znanosti i umjetnosti*, 486, 57–76.
- BAZYLEV, B.A., POPEVIĆ, A., KARAMATA, S., KONONKOVA, N.N., SIMAKIN, S.G., OLUJIĆ, J., VUJNOVIĆ, L. & MEMOVIĆ, E. (2008): Mantle peridotites from the Dinaridic ophiolite belt and the Vardar zone western belt, central Balkan: A petrological comparison.– *Lithos*, 108, 37–71.
- BECCALUVA, L., MACCIOTTA, G., PICCARDO, G.B. & ZEDA, O. (1989): Clinopyroxene composition of ophiolite basalts as petrogenetic indicator.– *Chemical Geology*, 77, 165–182.
- BELAK, M., PAMIĆ, J., KOLAR-JURKOVŠEK, T., PECSKAY, Z. & KARAN, D. (1995): Alpine low-grade regional metamorphic complex of Mt. Medvednica (northwest Croatia).– In: I. VLAHOVIĆ, I. VELIĆ & M. ŠPARICA (eds.): 1st Croatian Geological Congress Proceedings. Institute of Geology, Zagreb, 67–70 (in Croatian with English summary).
- BLOOMER, S.H., TAYLOR, B., MACLEOD, C.J., STERN, R.J., FRYER, P., HAWKINS, J.W. & JOHNSON, L. (1995): Early arc volcanism and the ophiolite problem; a perspective from drilling in the western Pacific.– In: B. TAYLOR & J. NATLAND (eds.): Active Margins and Marginal Basins of the Western Pacific. Geophysical Monograph, American Geophys Union, 88, 1–30.
- BORTOLOTTI, V., MARRONI, M., PANDOLFI, L., PRINCIPI, G. & SACCANI, E. (2002): Interaction between mid-ocean ridge and subduction magmatism in Albanian ophiolites.– *Journal of Geology*, 110, 561–576.
- BORTOLOTTI, V. & PRINCIPI, G. (2005): Tethyan ophiolites and Pangea break-up.– *Island Arc*, 14, 442–470.
- CHEN, C.Y., FREY, F.A. & GARCIA, M.O. (1990): Evolution of alkaline lavas at Haleakala Volcano, east Maui, Hawaii.– *Contributions to Mineralogy and Petrology*, 105, 197–218.
- CLAESON, D.T. & MEURER, W.P. (2004): Fractional crystallization of hydrous basaltic ‘arc-type’ magmas and the formation of amphibole-bearing gabbroic cumulates.– *Contributions to Mineralogy and Petrology*, 147, 288–304.
- CLAGUE, D.A. & FREY, F.A. (1982): Petrology and trace element geochemistry of the Honolulu Volcanism, Oahu: implications for the oceanic mantle below Hawaii.– *Journal of Petrology*, 23, 447–504.
- COLOMBI, A. (1989): Métamorphisme et Géochimie des roches mafiques des Alpes Ouest-centrales (géoprofil Viège-Domodossola-Locarno).– *Mémoires de Géologie (Lausanne)*, 4, 1–216.
- CONRAD, W.K. & KAY, R.W. (1984): Ultramafic and mafic inclusions from Adak Islands: Crystalization history, and implications for the nature of primary magmas and crustal evolution in the Aleutian arc.– *Journal of Petrology*, 25, 88–125.
- CONSTANTIN, M. (1999): Gabbroic intrusion and magmatic metasomatism in harzburgites from the Garrett transform fault: implication for the nature of the mantle-crust transitional fast-spreading ridges.– *Contributions to Mineralogy and Petrology*, 136, 111–130.
- COOGAN, L.A. (2003): Contamination of the lower oceanic crust in the Oman ophiolite.– *Geology*, 3, 1065–1068.
- COOGAN, L.A., WILSON, R.N., GILLIS, K.M. & MACLEOD, C.J. (2001): Near-solidus evolution of oceanic gabbros: insights from amphibole geochemistry.– *Geochimica et Cosmochimica Acta*, 65, 4339–4357.
- COUSENS, B.L., ALLAN, J.F. & GORTON, M.P. (1994): Subduction-modified pelagic sediments as the enriched component in back-arc basalts from the Japan Sea: Ocean Drilling Program Sites 797 and 794.– *Contributions to Mineralogy and Petrology*, 117, 421–434.
- COX, K.G., BELL, J.D. & PANKHUST, R.J. (1979): The interpretation of igneous rocks.– London, UK: George Allen and Unwin, 450 p.
- CRNKOVIĆ, B., BABIĆ, V. & TOMAŠIĆ, I. (1974): The gabbro of Hrušovec near Ljubešćica on mount Kalnik (Northern Croatia).– *Geološki vjesnik*, 27, 153–171 (in Croatian with English summary).
- DEBARI, S.M. & COLEMAN, R.G. (1989): Examination of deep levels of an island arc: Evidence from the Tonsina ultramafic-mafic assemblage, Tonsina, Alaska.– *Journal of Geophysical Research*, 94, 4373–4391.
- ERNST, W.G. & LIU, J. (1998): Experimental phase-equilibrium study of Al- and Ti-contents of calcic amphibole in MORB – A semi-quantitative thermobarometer.– *American Mineralogist*, 83, 952–969.

- EWART, A., BRYAN, W.B., CHAPPELL, B.W. & RUDNICK, R.L. (1994): 24. Regional geochemistry of the Lau-Tonga arc and back arc system.– In: J. HAWKINS, L. PARSON & J. ALLAN (eds.): The Ocean Drilling Program Proceedings, Scientific Results, 135, 385–425.
- EWART, A., COLLERSON, K.D., REGELOUS, M., WENDT, J.I. & NIU, Y. (1998): Geochemical evolution within the Tonga-Kermadec-Lau arc-back-arc system: the role of varying mantle wedge composition in space and time.– *Journal of Petrology*, 39, 331–368.
- FESTA, A., PINI, G.A., DILEK, Y. & CODEGONE, J. (2010): Mélanges and mélange-forming processes: a historical overview and new concepts.– In: Y. DILEK (ed.): *Alpine Concept in Geology*. *International Geology Review*, 52, 1040–1105.
- GESHI, N., UMINO, S., KUMAGAI, H., SINTON, J.M., WHITE, S.M., KISIMOTO, K. & HILDE, T.W. (2007): Discrete plumbing systems and heterogeneous magma sources of a 24 km³ off-axis lava field on the western flank of East Pacific Rise, 14° S.– *Earth and Planetary Science Letters*, 258, 61–72.
- GORIČAN, Š., HALAMIĆ, J., GRGASOVIĆ, T. & KOLAR-JURKOVŠEK, T. (2005): Stratigraphic evolution of Triassic arc-backarc system in northwestern Croatia.– *Bulletin de la Societe Géologique de France*, 176, 3–22.
- GRIBBLE, R.F., STERN, R.J., NEWMAN, S., BLOOMER, S.H. & O'HEARN, T. (1998): Chemical and isotopic composition of lavas from the northern Mariana trough: implications for magmatogenesis in back-arc basins.– *Journal of Petrology*, 39, 125–154.
- HAAS, J., MIOČ, P., PAMIĆ, J., TOMLJENOVIĆ, B., ÁRKAI, P., BÉRCZI-MAKK, A., KOROKNAI, B., KOVÁCS, S. & R-FELGENHAUER, E. (2000): Complex structural pattern of the Alpine-Dinaridic Pannonian triple junction.– *International Journal of Earth Sciences*, 89, 377–389.
- HAAS, J. & KOVÁCS, S. (2001): The Dinaridic-Alpine connection – as seen from Hungary.– *Acta Geologica Hungarica*, 44, 345–362.
- HALAMIĆ, J. (1998): Lithostratigraphy of Jurassic and Cretaceous sediments with ophiolites from the Mts. Medvednica, Kalnik and Ivanščica. PhD Thesis, University of Zagreb, Zagreb, 188 p. (in Croatian with English summary).
- HALAMIĆ, J., SLOVENEK, D. & KOLAR-JURKOVŠEK, T. (1998): Triassic pelagic limestones in pillow lavas in the Orešje quarry near Gornja Bistra, Medvednica Mt. (Northwest Croatia).– *Geol. Croatica*, 51, 33–45.
- HÉBERT, R.M., CONSTANTIN, M. & ROBINSON, P.T. (1991): Primary mineralogy of Leg 118 gabbroic rocks and their place in the spectrum of oceanic mafic igneous rocks.– In: R.P. VON HERZEN, P.T. ROBINSON et al. (eds.): *The Ocean Drilling Program Proceedings*, Scientific Results, 118, 3–20.
- IGNJATIĆ, S. (2007): Upper Cretaceous amphibolites from Iherzolite metamorphic sole (Kalnik Mt., Croatia).– Unpubl. B.Sc Thesis, University of Zagreb, Zagreb, 61 p. (in Croatian with English summary).
- INSERGUEIX-FILIPPI, D., DUPEYRAT, L., DIMO-LAHITTE, A., VERGÉLY, P. & BÉBIEN, J. (2000): Albanian ophiolites. II – Model of subduction zone infancy at a mid-ocean ridge.– *Ofioliti*, 25, 47–53.
- JUDIK, K., RANTITSCH, G., RAINER, T.M., ARKAI, P. & TOMLJENOVIĆ, B. (2008): Alpine metamorphism of organic matter in metasedimentary rocks from Mt. Medvednica (Croatia).– *Swiss Journal of Geosciences*, 101, 605–616.
- KISS, G., MOLNÁR, F., PALINKAŠ, L., KOVÁCS, S. & HORVATOVIĆ, H. (2012): Correlation of Triassic advanced rifting-related Neotethyan submarine basaltic volcanism of the Darnó Unit (NE-Hungary) with some Dinaridic and Hellenidic occurrences on the basis of volcanological, fluid–rock interaction, and geochemical characteristics.– *Int. J. Earth Sci.*, 101, 1503–1521.
- KOCAK, K., ISIK, F., ARSLAN, M. & ZEDEF, V. (2005): Petrological and source region characteristics of ophiolitic hornblende gabbros from the Aksarav and Kavseri regions, central Anatolian crystalline complex, Turkey.– *Journal of Asian Earth Sciences*, 25, 883–891.
- KOSTOPOULOS, D.K. & JAMES, S.D. (1992): Parameterization of the melting regime of the shallow upper mantle and the effects of variable lithospheric stretching on mantle modal stratification and trace element concentrations in magmas.– *Journal of Petrology*, 33, 665–691.
- LEAKE, B.E. et al. (1997): Nomenclature of amphiboles: Report of the Subcommittee on amphiboles of the International Mineralogical Association, Commission on New Minerals and Mineral Names.– *Canadian Mineralogist*, 35, 219–246.
- LEAT, P.T., LIVERMORE, R.A., MILLAR, I.L. & PEARCE, J.A. (2000): Magma supply in back-arc spreading centre segment E2, East Scotia Ridge.– *Journal of Petrology*, 41, 845–866.
- LUDWIG, K. (2005): Isopleth/Ex v.3, USGS Open File report.
- LUGOVIĆ, B., ALTHERR, R., RACZEK, I., HOFMANN, A.W. & MAJER, V. (1991): Geochemistry of peridotites and mafic igneous rocks from the Central Dinaric Ophiolite Belt, Yugoslavia.– *Contributions to Mineralogy and Petrology*, 106, 201–216.
- LUGOVIĆ, B., ŠEGVIĆ, B. & ALTHERR, R. (2006): Petrology and tectonic significance of greenschists from the Medvednica Mts. (Sava unit, NW Croatia).– *Ofioliti*, 31, 39–50.
- LUGOVIĆ, B., SLOVENEK, D., HALAMIĆ, J. & ALTHERR, R. (2007): Petrology, geochemistry and geotectonic affinity of the Mesozoic ultramafic rocks from the southwesternmost Mid-Transdanubian Zone in Croatia.– *Geologica Carpathica*, 58, 511–530.
- MAHLBURG, V. & KAY, S. (1983): Metamorphism in the Aleutian arc: the Finger bay pluton, Adak, Alaska.– *Canadian Mineralogist*, 21, 665–681.
- MARTINEZ, F., OKINO, K., OHARA, Y., REYSENBACH, A.-M. & GOFFREDI, S.K. (2007): Back-arc basins.– *Oceanography*, 20, 117–127.
- MELI, S., MONTANINI, A., THÖNI, M. & FRANK, W. (1996): Age of granulite blocks from the external Liguride units (Northern Apennines, Italy).– *Memorie di Scienze Geologiche*, Padova, 48, 65–72.
- MCCULLOCH, M.T., GREGORY, R.T., WASSERBURG, G.J. & TAYLOR JR., H.P. (1981): Sm-Nd, Rb-Sr, and ¹⁸O/¹⁶O isotopic systematics in an oceanic crustal section: evidence from the Samail ophiolite.– *Journal of Geophysical Research*, 86, 2721–2735.
- MILLER, CH. & THÖNI, M. (1997): Eo-Alpine eclogitisation of Permian MORB-type gabbros in the Koralpe (Eastern Alps, Austria): new geochronological, geochemical and petrological data.– *Chemical Geology*, 137, 283–310.
- MORIMOTO, N. (1988): Nomenclature of pyroxenes.– *Schweizerische Mineralogische und Petrographische Mitteilungen*, 68, 95–111.
- PALINKAŠ, L.A., KOLAR-JURKOVŠEK, T., BOROJEVIĆ, S. & BERMANEC, V. (2000): Triassic rifting magmatism within Zagorje-Mid-Transdanubian Zone, exemplified by pillow lavas of Hruškovec, Mt. Kalnik, N. Croatia, PANCARDI 2000 Meeting.– *Geološke vijesti*, 37, 98–99.
- PALINKAŠ, L.A., BERMANEC, V., MORO, A., DOGANČIĆ, D. & STRMIĆ-PALINKAŠ, S. (2006): The northernmost Ni-lateritic weathering crust in the Tethyan domain, Gornje Orešje, Medvednica Mt., Mesozoic ophiolite belts of northern part of the Balkan.– *Balkan Peninsula Proceedings*, 97–101.
- PALINKAŠ, L.A., BERMANEC, V., BOROJEVIĆ-ŠOŠTARIĆ, S., KOLAR-JURKOVŠEK, T., STRMIĆ-PALINKAŠ, S., MOLNÁR, F. & KNIEWALD, G. (2008): Volcanic facies analysis of a subaqueous basalt lava-flow complex at Hruškovec, NW Croatia – evidence of advanced rifting in the Tethyan domain.– *J. Volc. Geotherm. Res.* 178, 644–656.

- PAMIĆ, J. (1997): The northwesternmost outcrops of the Dinaridic ophiolites: a case study of the Mt. Kalnik (North Croatia).— *Acta Geologica Hungarica*, 40, 37–56.
- PAMIĆ, J. (2000): The Periadriatic-Sava-Vardar Suture Zone.— In: I. VLAHOVIĆ & R. BIONDIĆ (eds.): 2nd Croatian Geological Congress Proceedings. Institute of Geology, Zagreb, 333–337 (in Croatian with English summary).
- PAMIĆ, J. (2002): The Sava-Vardar Zone of the Dinarides and Hellenides versus the Vardar ocean.— *Eclogae Geologicae Helvetiae*, 95, 99–113.
- PAMIĆ, J. & TOMLJENOVIĆ, B. (1998): Basic geological data on the Croatian part of the Mid-Transdanubian Zone as exemplified by Mt. Medvednica located along the Zagreb-Zemlen Fault Zone.— *Acta Geologica Hungarica*, 41, 389–400.
- PAMIĆ, J., TOMLJENOVIĆ, B. & BALEN, D. (2002): Geodynamic and petrogenetic evolution of Alpine ophiolites from the central and NW Dinarides: an overview.— *Lithos*, 65, 113–142.
- PEARCE, J.A. (1983): Role of the sub-continental lithosphere in magma genesis at active continental margins.— In: C.J. HAWKESWORTH & M.J. NORRY (eds.): *Continental basalts and mantle xenoliths*. Nantwich, UK: Shiva, 230–249.
- PEARCE, J.A., LIPPARD, S.J. & ROBERTS, S. (1984): Characteristics and tectonic significance of supra-subduction zone ophiolites.— In: B.P. KOKELAAR & M.F. HOWELLS (eds.): *Marginal Basin Geology*, Geol Soc London, Special Publications, 16, 17–94.
- PEARCE, J.A., BAKER, P.E., HARVEY, P.K. & LUFF, I.W. (1995): Geochemical evidence for subduction fluxes, mantle melting for fractional crystallization beneath the South Sandwich island arc.— *Journal of Petrology*, 36, 1073–1109.
- PEATE, D.W., PEARCE, J.A., HAWKESWORTH, C.J., COLLEY, H., EDWARDS, M.H. & HIROSE, K. (1997): Geochemical variations in Vanuatu arc lavas: the role of subducted material and a variable mantle wedge composition.— *Journal of Petrology*, 38, 1331–1358.
- POLJAK, J. (1942): A contribution to the knowledge of geology of the Mt. Kalnik.— *Vjestnik Hrvatskog Državnog Geološkog Zavoda i Hrvatskog Državnog Geološkog Muzeja*, 1, 53–92 (in Croatian with German summary).
- POUCHOU, J.L. & PICOIR, F. (1984): A new model for quantitative analyses. I. Application to the analysis of homogeneous samples.— *La Recherche Aérospatiale*, 3, 13–38.
- POUCHOU, J.L. & PICOIR, F. (1985): “PAP” (ϕ - ρ -Z) correction procedure for improved quantitative microanalysis.— In: J.T. Armstrong (ed.): *Microbeam Analysis*, San Francisco, California, USA: San Francisco Press, 104–106.
- RENNE, P.R., MUNDIL, R., BALCO, G., MIN, K. & LUDWIG, K.R. (2010): Joint determination of ^{40}K decay constants and $^{40}\text{Ar}^*/^{40}\text{K}$ for the Fish Canyon sanidine standard, and improved accuracy for $^{40}\text{Ar}/^{39}\text{Ar}$ geochronology.— *Geochimica et Cosmochimica Acta*, 74, 5349–5367.
- RENNE, P.R., MUNDIL, R., BALCO, G., MIN, K. & LUDWIG, K.R. (2011): Response to the Comment by W. H. SCHWARZ et al. on “Joint determination of ^{40}K decay constants and $^{40}\text{Ar}/^{40}\text{K}$ for the Fish Canyon sanidine standard, and improved accuracy for $^{40}\text{Ar}/^{39}\text{Ar}$ geochronology” by P.R. RENNE et al. (2010).— *Geochimica et Cosmochimica Acta*, 75, 5097–5100.
- ROBERTSON, A., KARAMATA, S. & ŠARIĆ, K. (2009): Overview of ophiolites and related units in the late Palaeozoic-early Cenozoic magmatic and tectonic development of Tethys in the northern part of the Balkan region.— *Lithos*, 108, 1–36.
- SACCANI, E., BECCALUVA, L., PHOTIADES, A. & ZEDA, O. (2011): Petrogenesis and tectono-magmatic significance of basalts and mantle peridotites from the Albanian-Greek ophiolites and sub-ophiolitic mélanges. New constraints for the Triassic-Jurassic evolution of the Neo-Tethys in the Dinaride sector.— *Lithos*, 124, 227–242.
- SCHMID, S.M., BERNOULLI, D., FÜGENSCHUH, B., MATENCO, L., SCHEFFER, S., SCHUSTER, R., TISCHLER, M. & USTASZEWSKI, K. (2008): The Alpine-Carpathian-Dinaridic orogenic system: correlation and evolution of tectonic units.— *Swiss Journal of Geoscience*, 101, 139–183.
- SCHWARZ, W.H., KOSSERT, K., TRIELOFF, M. & HOPP, J. (2011): Comment on the “Joint determination of ^{40}K decay constants and $^{40}\text{Ar}^*/^{40}\text{K}$ for the Fish Canyon sanidine standard, and improved accuracy for $^{40}\text{Ar}/^{39}\text{Ar}$ geochronology” by Paul R. RENNE et al. (2010).— *Geochimica et Cosmochimica Acta*, 75, 5094–5096.
- SCHWARZ, W.H. & TRIELOFF, M. (2007): Intercalibration of ^{40}Ar - ^{39}Ar age standards NL-25, HB3gr hornblende, GA1550, SB-3HD-B1 biotite and BMus/2 muscovite.— *Chemical Geology*, 242, 218–231.
- SERRI, G. & SAITTA, M. (1980): Fractionation trends of gabbroic complexes from high-Ti and low-Ti ophiolites and from the crust of major oceanic basins: a comparison.— *Ophioliti*, 5, 241–264.
- SERRI, S. (1981): The petrochemistry of ophiolitic gabbro-complexes: A key for classification of ophiolites to low-Ti and high-Ti types.— *Earth and Planetary Science Letters*, 52, 203–212.
- SHERVAIS, J.W. (1982): Ti-V plots and petrogenesis of modern and ophiolitic lavas.— *Earth and Planetary Science Letters*, 59, 101–118.
- SHERVAIS, J.W. (2001): Birth, death, and resurrection: The Life cycle of supra-subduction zone ophiolites.— *Geochemistry, Geophysics, Geosystems*, 2, 1010, 45 p. [doi: 10.1029/2000GC000080].
- SINTON, J.M., FORD, L., CHAPPELL, B. & MCCULLOCH, M. (2003): Magma genesis and mantle heterogeneity in the Manus back-arc basin, Papua New Guinea.— *Journal of Petrology*, 44, 159–195.
- SLOVENEK, DA. & LUGOVIĆ, B. (2008): Amphibole gabbroic rocks from the Mt. Medvednica ophiolite mélange (NW Croatia): geochemistry and tectonic setting.— *Geologica Carpathica*, 59, 277–293.
- SLOVENEK, DA. & LUGOVIĆ, B. (2009): Geochemistry and tectono-magmatic affinity of extrusive and dyke rocks from the ophiolite mélange in the SW Zagorje-Mid-Transdanubian Zone (Mt. Medvednica, Croatia).— *Ophioliti*, 34, 63–80.
- SLOVENEK, DA. & LUGOVIĆ, B. (2012): Evidence of the spreading culmination in the Eastern Tethyan Repno oceanic domain assessed by the petrology and geochemistry of N-MORB extrusive rocks from the Mt. Medvednica ophiolite mélange (NW Croatia).— *Geologia Croatica*, 65, 435–446.
- SLOVENEK, DA., LUGOVIĆ, B. & VLAHOVIĆ, I. (2010): Geochemistry, petrology and tectonomagmatic significance of basaltic rocks from the ophiolite mélange at the NW External-Internal Dinarides junction (Croatia).— *Geologica Carpathica*, 61, 273–294.
- SLOVENEK, DA., LUGOVIĆ, B., MEYER, H-P. & GARAPIĆ-ŠIFTAR, G. (2011): A tectono-magmatic correlation of basaltic rocks from ophiolite mélanges at the north-eastern tip of the Sava-Vardar suture Zone, Northern Croatia, constrained by geochemistry and petrology.— *Ophioliti*, 36, 77–100.
- SÖLVA, H., GRASEMANN, B., THÖNI, M., THIEDE, R. & HABLER, G. (2005): The Schneeberg Normal Fault Zone: Normal faulting associated with Cretaceous SE-directed extrusion in the Eastern Alps (Italy/Austria).— *Tectonophysics*, 401, 143–166.
- STAMPFLI, G.M. & BOREL, G.D. (2002): A plate tectonic model for the Paleozoic and Mesozoic constrained by dynamic plate boundaries and restored synthetic ocean isochrons.— *Earth and Planetary Science Letters*, 196, 17–33.
- STAMPFLI, G.M. & BOREL, G.D. (2004): The TRANSMED transects in space and time: constraints on the paleotectonic evolution of the Mediterranean domain.— In: W. CAVAZZA, F. ROURE, W. SPACKMAN, G.M. STAMPFLI & P.A. ZIEGLER (eds.): *The TRANSMED Atlas: the Mediterranean Region from crust to mantle*. Heidelberg, Germany, Springer, 53–80.

- STEIGER, R.H. & JÄGER, E. (1977): Subcommittee on Geochronology: convention on the use of decay constants in geo- and cosmochronology.– *Earth and Planetary Science Letters*, 36, 359–362.
- STERN, C. (1979): Open and closed system igneous fractionation within two Chilean ophiolites and tectonic implication.– *Contributions to Mineralogy and Petrology*, 68, 243–258.
- STERN, C. (2004): Subduction initiation: spontaneous and induced.– *Earth and Planetary Science Letters*, 226, 275–292.
- STERN, R.J. & BLOOMER, S.H. (1992): Subduction zone infancy: Examples from the Eocene Izu-Bonin-Mariana and Jurassic California arcs.– *Geological Society of America Bulletin*, 104, 1621–1636.
- STERN, R.J., BLOOMER, S.H., MARTINEZ, F., YAMAZAKI, T. & HARRISON, T.M. (1996): The composition of back-arc basin lower crust and upper mantle in the Mariana Trough: A first report.– *Island Arc*, 5, 354–372.
- SUN, S.S. & MCDONOUGH, W.F. (1989): Chemical and isotopic systematics of oceanic basalts: implications for mantle composition and processes.– In: A.D. SAUNDERS & M.J. NORRIS (eds.): *Magmatism in ocean basins*. Geological Society of London, Special Publications, 42, 313–345.
- ŠIMUNIĆ, AN. & PAMIĆ, J. (1989): Ultramafic rocks from the neighbourhood of Gornje Orešje on the northwestern flanks of Mt. Medvednica (northern Croatia).– *Geološki vjesnik*, 42, 93–101.
- ŠIMUNIĆ, AN., PIKIJA, M., HEĆIMOVIĆ, I. & ŠIMUNIĆ, AL. (1981): Osnovna geološka karta SFRJ 1:100000. Tumač za list Varaždin [*Basic Geological Map of SFRY 1:100000, Geology of the Varaždin sheet* – in Croatian].– Institut za geološka istraživanja Zagreb, Savezni geološki zavod Beograd, 1–81.
- ŠIMUNIĆ, AN., PIKIJA, M. & HEĆIMOVIĆ, I. (1982): Osnovna geološka karta SFRJ 1:100000, list Varaždin [*Basic Geological Map of SFRY 1:100000, Varaždin sheet* – in Croatian].– Institut za geološka istraživanja Zagreb, Savezni geološki zavod Beograd.
- ŠIMUNIĆ, AN., NAJĐENOVSKI, J. & PAMIĆ, J. (1993): Chaotic rock complexes – possible hydrocarbon accumulations in South-Western parts of the Pannonian Basin (Republic of Croatia).– *Nafta*, 44, 609–616.
- TARI, V. & PAMIĆ, J. (1998): Geodynamic evolution of the Northern Dinarides and the southern parts of the Pannonian Basin.– *Tectonophysics*, 297, 296–281.
- TATSUMI, Y. & EGGINS, S. (1995): *Subduction zone magmatism*.– Cambridge, Massachusetts, USA, Blackwell, 221 p.
- TOMLJENOVIĆ, B., CSONTOS, L., MÁRTON, E. & MÁRTON, P. (2008): Tectonic evolution of the northwestern Internal Dinarides as constrained by structures and rotation of Medvednica Mountains, North Croatia.– *Geological Society London, Special Publications*, 298, 145–167.
- TRIBUZIO, R., TIEPOLO, M. & THIRLWALL, M.F. (2000): Origin of titanian pargasite in gabbroic rocks from the Northern Apennine ophiolites (Italy): insights into the late-magmatic evolution of a MOR-type intrusive sequence.– *Earth and Planetary Science Letters*, 176, 281–293.
- TRUBELJA, F., MARCHING, V., BURGATH, K-P. & VUJOVIĆ, Ž. (1995): Origin of the Jurassic Tethyan ophiolites in Bosnia: a geochemical approach to tectonic setting.– *Geologia Croatica*, 48, 49–66.
- USTASZEWSKI, K., SCHMID, S.M., LUGOVIĆ, B., SCHUSTER, R., SCHALTEGGER, U., BERNOULLI, D., HOTTINGER, L., KOUNOV, A., FÜGENSCHUH, B. & SCHEFER, S. (2009): Late Cretaceous intra-oceanic magmatism in the internal Dinarides (northern Bosnia and Herzegovina): Implications for the collision of the Adriatic and European plates.– *Lithos*, 108, 106–125.
- VLAHOVIĆ, I., TIŠLJAR, J., VELIĆ, I. & MATIČEC, D. (2005): Evolution of the Adriatic carbonate platform: palaeogeography, main events and depositional dynamics.– *Palaeogeography, Palaeoclimatology Palaeoecology*, 220, 333–360.
- VRKLJAN, M. (1989): *Eruptive rocks from Mt. Kalnik*.– Unpubl. PhD Thesis, University of Zagreb, Zagreb, 94 p. (in Croatian with English summary).
- VRKLJAN, M. & GARAŠIĆ, V. (2004): Different geochemical signatures developed in some basic magmatic rocks of Mt. Kalnik (North Croatia).– *Rudarsko-geološko-naftni zbornik*, 16, 65–73.
- WAKABAYASHI, J. & DILEK, Y. (2000): Spatial and temporal relationships between ophiolites and their metamorphic soles: a test of model of forearc ophiolite genesis.– In: Y. DILEK, E.M. MOORE, D. ELTHON & A. NICOLAS (eds.): *Ophiolites and oceanic crust: New insights from field studies and the ocean drilling program*: Boulder, Colorado. The Geological Society of America, Special Paper, 349, 53–64.
- WAKABAYASHI, J. & DILEK, Y. (2003): What constitutes “emplacement” of an ophiolite?: mechanisms relationship to subduction initiation and formation of metamorphic soles.– In: Y. DILEK & P.T. ROBINSON (eds.): *Ophiolites in Earth history*. Geological Society London, Special Publication, 218, 427–447.
- WHATAM, S.A. & STERN, R.J. (2011): The ‘subduction initiation rule’: a key for linking ophiolites, intra-oceanic forearcs, and subduction initiation.– *Contributions to Mineralogy and Petrology*, 162, 1031–1045.
- WILSON, M. (1989): *Igneous petrogenesis*.– London, UK, Unwin Hyman Ltd., 466 p.
- WOOD, D.A. (1980): The application of a Th-Hf-Ta diagram to problems of tectonomagmatic classification and establishing the nature of crustal contamination of basaltic lavas of the British Tertiary volcanic province.– *Earth and Planetary Science Letters*, 50, 11–30.
- ZANE, A. & WEISS, Z. (1998): A procedure for classifying rock-forming chlorites based on microprobe data.– *Rendiconti Lincei Scienze Fisiche e Naturali*, 9, 51–56.
- ZINDLER, A. & HART, S.R. (1986): Chemical geodynamics.– *Annual Review of Earth and Planetary Sciences*, 14, 439–571.

Manuscript received July 24, 2014

Revised manuscript accepted January 23, 2015

Available online February 27, 2015